Speed Estimation Techniques for Sensorless Vector Control of Induction Motor

A DISSERTATION

Submitted in partial fulfillment of the

requirements for the award of degree

of

INTEGRATED DUAL DEGREE WITH B.TECH IN ELECTRICAL ENGINEERING

AND M.TECH IN POWER ELECTRONICS

BY

ATINDERPAL SINGH

11212003

DEPARTMENT OF ELECTRICAL ENGINEERING

INDIAN INSTITUTE OF TECHNOLOGY ROORKEE

ROORKEE – 247667

May 2016

CANDIDATE'S DECLARATION

I hereby declare that the work, which is being presented in this report entitled "**Speed Estimation Techniques for Sensorless Vector Control of Induction Motor**" in partial fulfilment of requirement for the award of degree of Master of technology in Electrical Engineering with socialization in Electric Drives & Power Electronics, and submitted in the Department of electrical Engineering of indian institute of technology Roorkee, India, is an authentic record of my own work carried out during the period from June 2015 to December 2015, under the supervision of Dr. S. P. Srivastava, Professor, Department of Electrical Engineering, of Indian Institute of Technology Roorkee, India.

The matter embodied in this report has not been submitted by me for the award of any other degree of this or any other Institute/ University.

Date: ATINDERPAL SINGH

Place: Roorkee

CERTIFICATE

This is to certify that the statement made by the candidate is correct to the best of knowledge and belief.

Dr. S. P. Srivastava

Professor

Department Of Electrical Engineering

Indian Institute of Technology, Roorkee

ROORKEE – 247667

ACKNOWLEDGEMENT

I take this opportunity to express my sincere gratitude towards my respected guide Dr. S. P. Srivastava, Professor, Department of Electrical Engineering, Indian Institute of Technology Roorkee, for their intuitive and meticulous guidance and perpetual inspiration in completion of report. I want to express my profound gratitude for his co-operation in scrutinizing the manuscript and his valuable suggestions throughout the work.

I would like to mention my parents for their endless support and encouragement and always believing and helping me to believe, that I can succeed at anything.

Acknowledgement would be incomplete without a word of gratitude to all my student friends for their timely help, encouragement and contribution in making it possible.

Dated: ATINDERPAL SINGH

Place: Roorkee Enrolment No. 11212003

ABSTRACT

The most frequently used electrical machine in various modern high-performance drive applications is the induction motor (IM), especially its squirrel cage type rotor counterpart. For the induction motor controlling to achieve variable speed, Vector Control (VC) or Field Oriented Control (FOC) have become the industrial standard. The vector control technique decouples the two component of stator current: one is responsible for controlling torque and other is controlling flux independently as in the case of separately excited fully compensated DC motor.

The closed loop control of Vector control of IM drives required accurate information of speed or rotor position. This information is provided by Tacho -generator or encoder. However the use of speed sensors has many drawbacks such as, higher cost, lower reliability, increase in weight and size and difficulty to use in harsh environment. These drawbacks of speed sensors can be eliminated by using sensorless speed estimation algorithms for induction motor drive.

Various speed sensorless techniques are presented, among which MRAS based speed observers offer simple implementation and require less computational effort compared to other methods. Various MRAS based observers have been introduced based on speed tuning signal such as the rotor flux, back e.m.f and reactive power.

Steady state and dynamic response of indirect vector control under various operating condition such as starting, reference speed change, load application and load removal for both with and without speed sensor is simulated and examined in MATLAB environment using Simulink and power system toolboxes. The performance of the different speed estimation techniques on the induction motor drive is compared and also their sensitivity towards stator resistance variations is tested. The analysis has been carried out on the basis of result obtained by numerical simulations. The simulation and evaluation of both control technique are performed using voltage source inverter fed three phase squirrel cage induction motor of 2HP rating.

List of Nomenclatures

OPERATOR	NAME
$\mathbf{i_{as}, i_{bs}, i_{cs}}$	Stator currents
$\mathbf{i_{ar}, i_{br}, i_{cr}}$	Rotor currents
$\mathbf{\bar{I}_s, \bar{I}_r}$	Stator and rotor current vectors
$\mathbf{\bar{V}_s, \bar{V}_r}$	Stator and rotor voltage vectors
$\mathbf{v_{as}, v_{bs}\ v_{cs}}$	Stator voltages
$\mathbf{i_{qs}, i_{ds}}$	Quadrature and direct axis stator current component
$\mathbf{i_{qr}, i_{dr}}$	Quadrature and direct axis rotor current component
$\omega_{\mathbf{r}}$	Rotor speed (rad/sec)
$\omega_{\mathbf{e}}$	Synchronous speed (rad/sec)
$\omega_{\mathbf{sl}}$	Slip speed (rad/sec)
ω_{base}	Base speed of motor
$\omega_{\mathbf{er}}$	Speed error between reference and actual
$\mathbf{i_{mr}}$	Excitation current
$\Psi_{\mathbf{s}}$	Stator flux linkage
$\Psi_{\mathbf{ds}}, \Psi_{\mathbf{qs}}$	Direct and quadrature component of stator flux linkage
$\Psi_{\mathbf{r}}$	Rotor flux linkage
$\Psi_{\mathbf{dr}}, \Psi_{\mathbf{qr}}$	Direct and quadrature component of rotor flux linkage
$\boldsymbol{\gamma_{sr}}$	Angle between stator and rotor flux in space

θ_{fs}, θ_{fr}	Angle between stator flux and d-axis and angle between rotor flux and d-axis
L_{ls}, L_{lr}	Leakage inductance of stator and rotor
L_m	Mutual inductance
L_s, L_r	Stator and rotor self-inductance
R_s, R_s	Stator and rotor resistance
τ_s, τ_r	Stator and rotor time constant
$\sigma = 1 - \frac{L_m^2}{L_s L_r}$	Total leakage factor
T_{em}	Electromagnetic torque
θ_e	Position angle of synchronously rotating frame
J	Moment of inertia

List of Figures

List of Tables

CONTENTS

CHAPTER 1 INTRODUCTION

1.1 GENERAL

Industry depends critically on the ability to move systems efficiently and precisely. The conversion of electrical energy to produce motion and torque has been the purview of motors for more than a century. But, the introduction of power electronic drives with motors has led to new design opportunities; the increased integration of drives and machines in recent years has created a quantum leap in productivity, efficiency, and system performance.

Variable speed operation of Induction motor drives can be generally classified as scalar control and vector control. Scalar control is used for low performance drives where only the magnitude and frequency of stator voltage or current is regulated. The most commonly used scalar control technique is the constant volts/Hertz (V/f) control, which offers moderate dynamics performance and is therefore used in application where high speed precision is not required such as fans, pumps and elevators. These control methods results in poor torque and flux response. High performance induction motor drive can be implemented by using vector control.

Vector control addresses this issue by resolving current phasor along rotor flux linkages. By resolving current phasor along rotor flux linkages, the control of ac machine becomes very similar to that of separately-excited dc machine. The component along the rotor flux linkage is field-producing current and component normal to rotor-flux linkage is the torque-producing current. But this requires the position of rotor flux linkages at every instant. This is achieved by voltage and current equations or by measuring with hall sensors. However the use of speed sensors has many drawbacks such as, higher cost, lower reliability, increase in weight and size and difficulty to use in harsh environment.

Speed sensorless techniques are developed to overcome the disadvantages of using sensors in high performance industrial applications. Various speed sensorless techniques are presented, among these schemes MRAS aped observers offer simple implementation and require less computational effort compared to other methods. Open-loop estimators and various MRAS observers have been introduced based on speed tuning signal as the rotor flux, back-emf and reactive power. The integrator present in the reference model of MRAS, variation of machine parameters with temperature and frequency, acquisition error of stator

voltage and currents during practical implementation result in inaccurate rotor speed/position estimation. The performance of the sensorless drive can be enhanced by eliminating these effects. An extensive literature review in the area of sensorless vector control techniques is presented below.

1.2 LITERATURE REVIEW

Variable speed operation of Induction motor drives can be divide into two major types : scalar control and vector control. The most commonly used scalar control technique is the constant volts/Hertz (V/f) control, in which the ratio of the magnitudes of the voltage and frequency is kept constant. As the rate of change of voltage and frequency has to be low, the transient performance of this control is poor [1-4].

The disadvantages of V/f control like sluggish response and poor dynamic performance were motivation for F. Blaschke [7] and W. Leonhard to introduce field-oriented control (FOC) for induction motor. This method comes with the revolution for controlling the speed of Induction motor drive in field of variable frequency variable speed drive which gives the excellent dynamic as well as steady state performance similar to a separately excited fully compensated dc motor. The main objective of FOC method is to get advantage of both the machine i.e. constructional feature of IM and controlling feature of separately excited fully compensated DC motor. This methodology gives independent control between flux and torque, and convert the non-linear control system into linear one [8].

The Mathematical modelling of IM is completed on the foundation of many developed theories [6]. The expansion in Power Electronics area [9], [16]-[19] has surfaced the way of real time execution of the vector control techniques [7]-[8], [12]-[15] of induction motor drive. The use of digital signal processors (DSPs) [9]-[10], [20]-[23], Microprocessors have made it promising to implement complex algorithm like FOC at a sensible cost. MATLAB with its toolboxes and Simulink have made the simulation much easier and modest.

Depending upon how the field angle is obtained the vector control technique is classified as direct vector control and indirect vector control techniques. In direct vector control, the unit vectors are obtained from rotor flux which can either be based on measurement or computation i.e. is based on stator equations of the machine [13]. In [14] different vector control structures and their suitability for reliable industrial drive system is discussed. In indirect vector control, the unit vectors are synthesized by the addition of the

rotor mechanical position vector and the command slip angle vector derived from the torque component of the current. In indirect vector control, the variations in rotor parameters due to temperature and saturation of rotor flux influences the accuracy of the speed and torque performance both in transient and in steady state [24].

In vector controlled AC drives the torque can be controlled in a manner similar to DC motor drives, but it requires accurate speed or position information for closed loop feedback control. This speed information is provided by an incremental encoder, which is the most common positioning transducer used in industrial applications. However the use of speed sensors has many drawbacks such as, higher cost, lower reliability, increase in weight and size, difficulty to use in harsh environment and inability to obtain high speed [25]-[28].

Various control algorithms for the elimination of the speed and position sensor have been proposed. Initially, these control algorithms estimated speed from instantaneous values of currents and voltages of the induction motor machine model. Various algorithms have been introduced using Model Reference Adaptive Systems [25], [31]-[33], [40, 41] Lueunberger and Kalman filter observers [34-35], and Artificial Intelligent techniques [36-37]. Most sensorless algorithms estimate speed from the voltage equations of the induction motor, hence they are sensitive to the electrical and mechanical parameters.

Various MRAS speed observers have been developed based on an error vector of speed tuning signal, they are rotor flux [25, 31-33], back e.m.f [38, 39] and reactive power [40, 41]. Among these rotor-flux based MRAS has high stator resistance parameter sensitivity while the reactive power MRAS is insensitive to stator resistance variations. Back e.m.f MRAS has low noise immunity due to differentiation as compared to others. Back e.m.f and reactive power MRAS have stability problems at low stator frequencies as the back e.m.f and reactive power quantities vanishes at low and zero speed.

In [42] the performance of the rotor flux and back-emf based MRAS observers are compared to test the sensitivity of both the techniques towards stator resistance variations. The back-e.m.f based MRAS is less parameter dependent as compared to the rotor-flux based MRAS. It also shows that back-e.m.f based MRAS besides having better tracking capability scheme, is more robust to parameters variations since no significant changes in estimated speed can be noted prior to the variations.

1.3 OBJECTIVE OF THE THESIS

This thesis presents a detailed study on the various aspects of the design and implementation of the Open-loop speed estimators and MRAS based observers for speed sensorless vector control of the induction motor drive. The thesis covers the following key areas:

- Modelling of the indirect vector control of the induction machine using dynamic equations of the induction machine in synchronously rotating reference frame.
- MATLAB simulation of the indirect vector control drive under various operating conditions to validate the indirect vector control model.
- Different algorithms to estimate rotor position using information from intsantaneous stator voltage and currents in combination with machine model for sensorless vector control of induction machine.
- Analysis of the open-loop estimators and MRAS based observers on the speed response of the indirect vector control drive and their sensitivity towards the motor parameter variations.
- MATLAB simulation work to compare the performance of the speed observers under various operating conditions of the drive.

CHAPTER 2: VECTOR CONTROL OF INDUCTION MOTOR

2.1 INTRODUCTION

Before the advent of vector control technique for induction motors, various control method ex: voltage control, frequency control, rotor resistance control, pole changing, Pole amplitude modulation technique, V/f control, flux control etc., have been used and named as scalar control. In scalar control particularly V/f control method [1-4], the motor is fed with variable frequency supply generated by an inverter controlled by Pulse Width Modulation (PWM) techniques. Here, the V/f ratio is maintained constant in order have constant torque throughout the operating range of the motor. Since only magnitudes of the input variable i.e. frequency and voltage are controlled, this is known as Scalar Control, such control techniques result in satisfactory response only in steady state conditions. The dynamic response of the drive from scalar control methods is observed to be sluggish. This is one of the major drawback of scalar control technique as applied to the induction motors.

With the advancement in the mathematical processing powers offered by the microcontrollers, advance control techniques are developed which use mathematical transformations to decouple the torque generating and flux producing functions in an AC induction machine. Such decoupled torque and magnetization control is commonly known as Vector Control or Field Oriented Control (FOC) [5, 7, 8].

Vector control of induction motor is similar to separately excited DC motor control in which flux and torque are controlled independently by decoupling the stator currents. The stator phase currents can be transformed from three-phase *abc* into *dq* axes currents in the synchronous frame using Parke's transformation:

$$\begin{bmatrix} i_{ds}^{e} \\ i_{qs}^{e} \end{bmatrix} = \frac{2}{3}\begin{bmatrix} \cos\theta_f & \cos(\theta_f - \frac{2\pi}{3}) & \cos(\theta_f + \frac{2\pi}{3}) \\ \sin\theta_f & \sin(\theta_f - \frac{2\pi}{3}) & \sin(\theta_f + \frac{2\pi}{3}) \end{bmatrix}\begin{bmatrix} i_{as}^{e} \\ i_{bs}^{e} \\ i_{cs}^{e} \end{bmatrix} \tag{2.1}$$

The stator current phasor and phase angle is defined as:

$$i_s = \sqrt{(i_{ds}^{e})^2 + (i_{qs}^{e})^2} \tag{2.2}$$

$$\theta_s = \tan^{-1}\left(\frac{i_{qs}^{e}}{i_{ds}^{e}}\right) \tag{2.3}$$

Where i_{ds}^{e} and i_{qs}^{e} are the components of the stator current phasor i_s along the dq axes in the rotating synchronous reference frame. The current phasor magnitude remains the same regardless of the reference frame chosen. Since the stator current produces both the rotor flux λ_r and the torque T_e, therefore the rotor flux producing component of current has to be in phase with λ_r . This stator current component resolved along λ_r is field producing component i_f and the perpendicular component is torque producing component i_T. Hence

$$\lambda_r \propto i_f \tag{2.4}$$

$$T_e \propto \lambda_r i_T \propto i_f i_T \tag{2.5}$$

The rotor flux phasor is rotating at a speed equal to the sum of the rotor and slip speeds, which is equal to the synchronous speed.

Vector control technique allows a squirrel-cage induction motor to be driven with high dynamic performance, comparable to that of a dc motor. This type of control is suitable for applications that require accurate control of speed and position. There are basically two different types of vector control techniques. Either direct or indirect field oriented control (FOC), depending upon the method of flux acquisition.

Direct Vector Control

In the direct method, the air-gap flux is directly measured with the help of sensors, search coils or taped stator windings or estimated from machine terminal variables such as stator voltage, current and speed. Since it is not possible to directly sense rotor flux, it is synthesized from the directly sensed air-gap flux. Rotor flux angle is directly computed from flux estimation or measurement.

A major drawback with the direct orientation scheme is the inherent problem at very low speeds when the machine IR drop dominates and the required integration of the signal to measure the air-gap flux is difficult. Fig. 2.1 shows the schematic drive scheme of an induction motor with impressed stator currents employing direct rotor flux-oriented control and using a voltage source inverter.

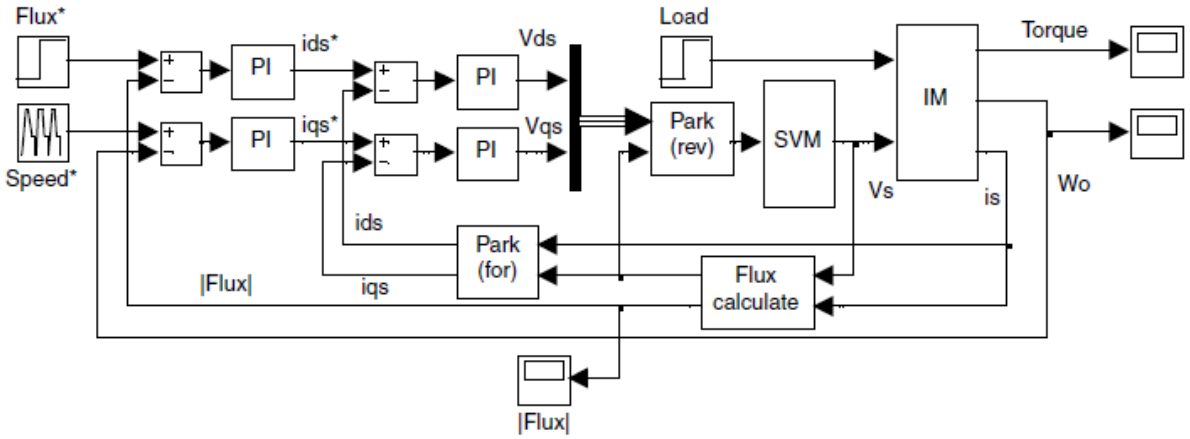

Fig. 2.1 Direct FOC of an induction motor

Indirect Vector Control

In this method, the rotor flux angle is indirectly computed by summing a sensed rotor position signal with a commanded slip position. In contrast to direct methods, the indirect methods are highly dependent on machine parameters, which may vary with temperature, saturation level and frequency. Consequently, parameter adaptation schemes are required to have a better overall performance.

1.2 CONCEPT OF VECTOR CONTROL AND ANALOGY

A control technique wherein two hypothetical, decoupled signals are produced, one responsible for the control of torque (i_{qs}^{*}) and the other for control of flux (i_{ds}^{*}) , so that the 3-ϕ Induction Motor behaves like a separately excited, fully compensated dc motor is referred as Vector Control (VC) or Field Oriented Control (FOC). This method gives an option to use induction motor in the industrial applications wherein four-quadrant operation with fast dynamics on a wide range of speed is required. The two decoupled signals of the stator current phasor are considered as control variables are expressed in d-q synchronously rotating reference current frame (SRRF). In this work rotor reference frame is considered, however in the later chapter, I will discuss about other possible reference frame and the reason of taking this reference frame. When the reference current signals generated by vector controller and the actual three phase current signals produced by induction motor (both in stationary reference frame) are identical to each other ,the vector control mode is said to be achieved.

The basic schematics of VCIMD shown in Fig.1.1. VCIMD system consist the synchronously rotating reference frame ($d^* - q^*$ axis) and the d^e axis is attached to the rotor flux vector ($\bar{\Psi}_r$) rotating at synchronous speed (ω_e). Consequent upon this, decoupling of the variables could be possible. So that, torque and flux can be separately controlled by two hypothetical current signal i.e. quadrature axis component (i_q^*) and direct axis component (i_d^*) respectively.

The feedback signals which is sensed from the machine is shaft speed (ω_r) and stator currents (i_{as} andi_{bs}). Reference speed (ω_r^*) and shaft speed (ω_r) is compared and error is computed, that error is passed through a suitable controller which will generate reference toque signal (T_{em}^*). Suitable value of excitation (i_{mr}^*) is generated by sensed shaft speed magnitude. T_{em}^* and i_{mr}^* act as two input which generate two hypothetical current signal (i_{qs}^* and i_{ds}^*), which independently responsible for controlling torque and flux of the drive.

ANALOGY

The analogy between the induction motor operated in vector control mode and fully compensated, separately excited dc motor can be deal with the help of fig.1.2. The equation of electromechanical torque for the dc motor is give as:

$$T_{em} = K_t * I_a * I_f \tag{2.1}$$

Where K_t= the torque constant of dc motor, I_a= Torque component of current and I_f= Field component of current.

As shown in fig.1.2, the two control signals of induction motors in SRRF (i_{qs}^* and i_{ds}^*) are analogous to field and armature component of current i.e. i_f and i_a respectively of DC motor. Therefore, the torque equation of an induction motor is expressed as:

$$T_{em}^* = K_{t1} * i_{qs}^* * i_{ds}^* \tag{1.2}$$

Where, K_{t1}= the torque constant of VCIMD, i_{qs}^*= Torque component of current and i_{ds}^*= Field component of current.

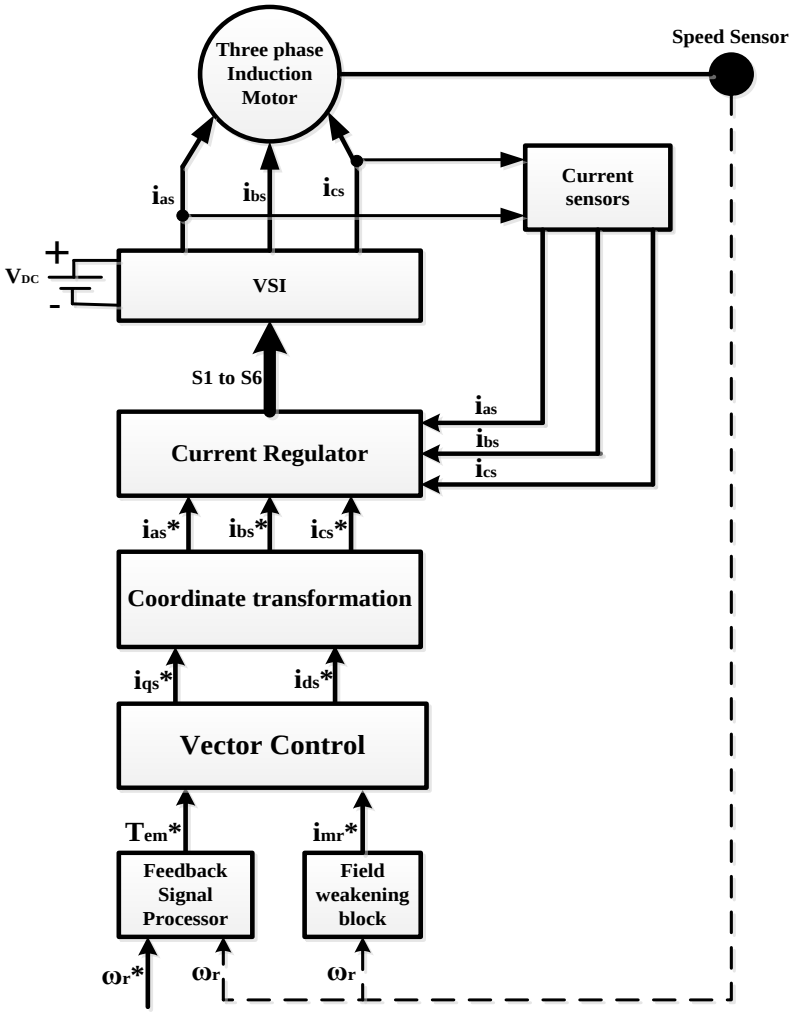

Fig.2.2 Basic block diagram of VCIMD

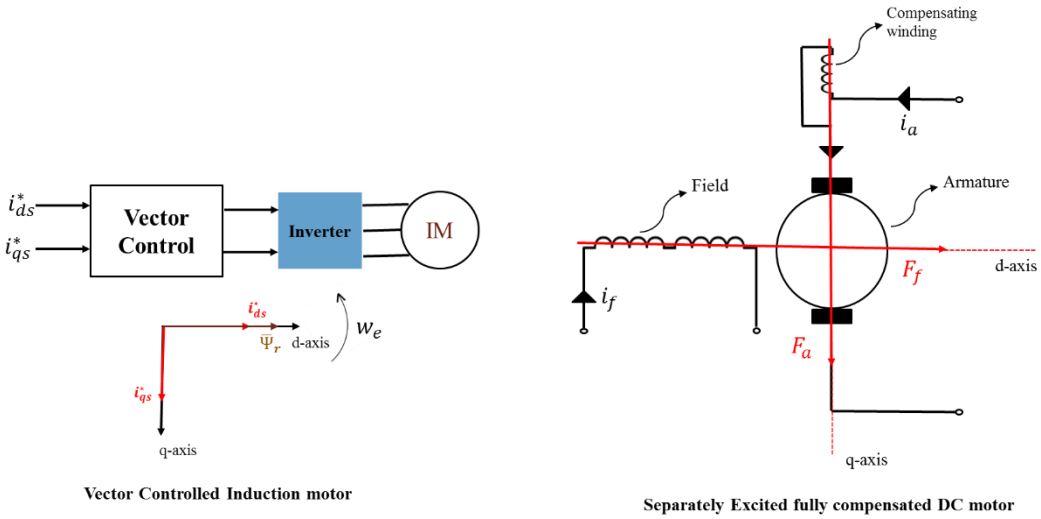

Fig. 2.3 VCIMD Analogy with DC Motor

Two torque equations 1.1 and 1.2, conclude that the Torque expressions are identical to each other. This shows that independent control can be achieve in case of induction motor by controlling it in SRRF. Therefore, the method known as Field Oriented Control (FOC) or Vector Control (VC) gives the induction motor control as separately excited, fully compensated DC motor.

The indirect vector control is widely used in high performance industrial application due its simplicity, fast dynamic response and eliminates the need of flux sensor or flux model but requires an accurate measurement of rotor position to calculate the precise position of rotor flux phasor. In this chapter the indirect vector control scheme is derived and modeled from rotor voltage equations.

2.3 INDIRECT VECTOR CONTROL MODELLING

Indirect Vector Control of induction machine is derived in synchronously rotating reference frame using dynamic equations of induction machine. The rotor equations of the induction machine containing flux linkages as variables are given as:

$$V_{dr}^{*} = 0 = R_r\, i_{dr}^{e} + p\, \Psi_{dr}^{e} - \omega_{sl}\, \Psi_{qr}^{e} \tag{2.6}$$

$$V_{qr}^{*} = 0 = R_r\, i_{qr}^{e} + p\, \Psi_{qr}^{e} + \omega_{sl}\, \Psi_{dr}^{e} \tag{2.7}$$

Where,

$$\omega_{sl} = \omega_s - \omega_r$$

$$\Psi_{dr}^{e} = L_r\, i_{dr}^{e} + L_m\, i_{ds}^{e} \tag{2.8}$$

$$\Psi_{qr}^{e} = L_r\, i_{qr}^{e} + L_m\, i_{qs}^{e}$$

To reduce the number of variables in the equation, the resultant rotor flux linkage 'Ψ_r' (also known as the rotor flux linkages phasor) is assumed to be on the direct axis as shown in fig.2.1. Also it corresponds with the reality that the rotor flux is a single variable. Hence, aligning the d-axis along the rotor flux phasor yields:

$$\Psi_r = \Psi_{dr}^{e}$$

$$\Psi_{qr}^{e} = 0 \tag{2.9}$$

$$p\Psi_{qr}^{e} = 0$$

Substituting (2.4) in (2.1) and (2.2) yields:

$$R_r\, i_{dr}^{e} + p\, \Psi_r = 0 \tag{2.10}$$

$$R_r\, i_{qr}^{e} + \omega_{sl}\, \Psi_r = 0 \tag{2.11}$$

The rotor currents in terms of stator quantities are expressed as:

$$i_{dr}^{e} = \frac{\Psi_r}{L_r} - \frac{L_m}{L_r}\, i_{ds}^{e} \tag{2.12}$$

$$i_{qr}^{e} = -\frac{L_m}{L_r}\, i_{qs}^{e} \tag{2.13}$$

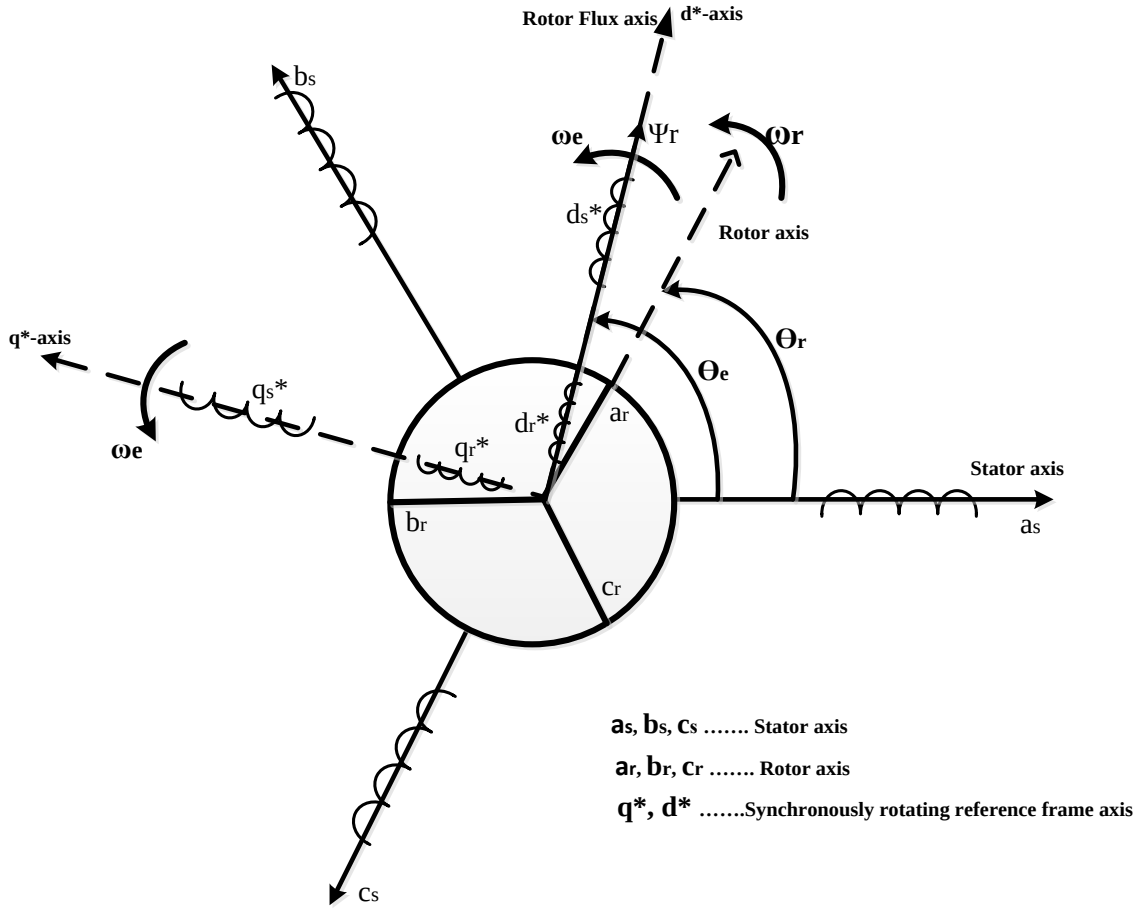

Fig.2.4 Space Phasor diagram of 3phase Induction motor (synchronously rotating d-q reference frame attached with rotor flux vector).

Substituting the above rotor currents equations into (2.5) and (2.6):

$$i_f = \frac{1}{L_m}\left[1 + T_r p\right] \Psi_r \tag{2.14}$$

$$\omega_{sl} = K_{it}\left[\frac{L_r}{T_r}\right]\left[\frac{T_e}{\Psi_r^2}\right] = \left[\frac{L_m}{T_r}\right]\left[\frac{i_T}{\Psi_r}\right] \tag{2.15}$$

Where $i_f = i_{ds}^e$, $i_T = i_{qs}^e$, $T_r = \frac{L_r}{R_r}$ and $K_{it} = \frac{2}{3}\frac{2}{P}$

The equation (2.9) resembles the field equation in a separately excited dc-machine. Similarly, by substituting the rotor currents in the torque expression, the electromagnetic torque is derived as:

$$T_e = \frac{3}{2}\frac{P}{2}\frac{L_m}{L_r}(i_{qs}^e \Psi_{dr}^e - i_{ds}^e \Psi_{qr}^e) \tag{2.16}$$

$$T_e = \frac{3}{2}\frac{P}{2}\frac{L_m}{L_r}\left(i_{qs}^e \Psi_r\right) = K_{te} i_{qs}^e \Psi_r = K_{te} \Psi_r i_T \tag{2.17}$$

Where $K_{te} = \frac{3}{2}\frac{P}{2}\frac{L_m}{L_r}$

From the above equation we can note that the torque is proportional to the product of the rotor flux linkages and the stator q-axis current. This is similar to the air gap torque expression of the dc machine, which is proportional to the product of the field flux and the armature current.

The *dq* components of stator reference currents (i_{ds}^e and i_{qs}^e) are converted back into reference *abc* phase-currents (i_{as}^* , i_{bs}^* and i_{cs}^*) using inverse Park's transformation as:

$$\begin{bmatrix} i_{as}^* \\ i_{bs}^* \\ i_{cs}^* \end{bmatrix} = \begin{bmatrix} \cos\theta_f & -\sin\theta_f \\ \cos(\theta_f - \frac{2\pi}{3}) & -\sin(\theta_f - \frac{2\pi}{3}) \\ \cos(\theta_f + \frac{2\pi}{3}) & -\sin(\theta_f + \frac{2\pi}{3}) \end{bmatrix} \begin{bmatrix} i_{ds}^e \\ i_{qs}^e \end{bmatrix} \tag{2.18}$$

Where θ_f is the electrical field angle of rotor flux linkage phasor and can be obtained as the sum of the rotor and slip angles:

$$\theta_f = \theta_r + \theta_{sl} = \int(\omega_r + \omega_{sl})dt \tag{2.19}$$

From these equations drive scheme is developed.

2.4 INDIRECT VECTOR CONTROL SCHEME

The vector controller receives the torque and flux requests to generate the torque and flux producing components of stator current and the slip angle θ_{sl} commands. From 2.9, 2.10 and 2.12 the commanded values of i_T, i_f and ω_{sl} are obtained as:

$$i_T^* = \frac{T_e^*}{K_{te}\Psi_r^*} = \frac{T_e^*}{\Psi_r^*}\frac{L_r^*}{L_m^*}\left(\frac{2}{3}\right)\left(\frac{2}{P}\right) = K_{it}\left(\frac{T_e^*}{\Psi_r^*}\right)\left(\frac{L_r^*}{L_m^*}\right) \tag{2.20}$$

$$i_f^* = (1 + T_r^* p)\frac{\Psi_r^*}{L_m^*} \tag{2.21}$$

$$\omega_{sl}^* = K_{it}\left[\frac{L_r^*}{T_r^*}\right]\left[\frac{T_e^*}{(\Psi_r^*)^2}\right] = K_{it}R_r^*\frac{T_e^*}{(\Psi_r^*)^2} = \frac{L_m^*}{T_r^*}\frac{i_T^*}{\Psi_r^*} \tag{2.22}$$

The command slip angle θ_{sl} is obtained by integrating ω_{sl}^*. The field angle is generated by summing the command slip angle and rotor angle. The three-phase stator current commands are generated from the torque and flux producing components (i_q^* and i_d^*) using dq to abc transformation as:

$$\begin{bmatrix} i_{as}^* \\ i_{bs}^* \\ i_{cs}^* \end{bmatrix} = \begin{bmatrix} \cos\theta_f & -\sin\theta_f \\ \cos(\theta_f - \frac{2\pi}{3}) & -\sin(\theta_f - \frac{2\pi}{3}) \\ \cos(\theta_f + \frac{2\pi}{3}) & -\sin(\theta_f + \frac{2\pi}{3}) \end{bmatrix} \begin{bmatrix} i_{ds}^* \\ i_{qs}^* \end{bmatrix} \tag{2.23}$$

The current commands are executed by the inverter with suitable control techniques. A block diagram below shows the realization of the indirect vector-control scheme. The implementation and simulation of the indirect vector-control scheme on an inverter fed induction motor is discussed in next chapter.

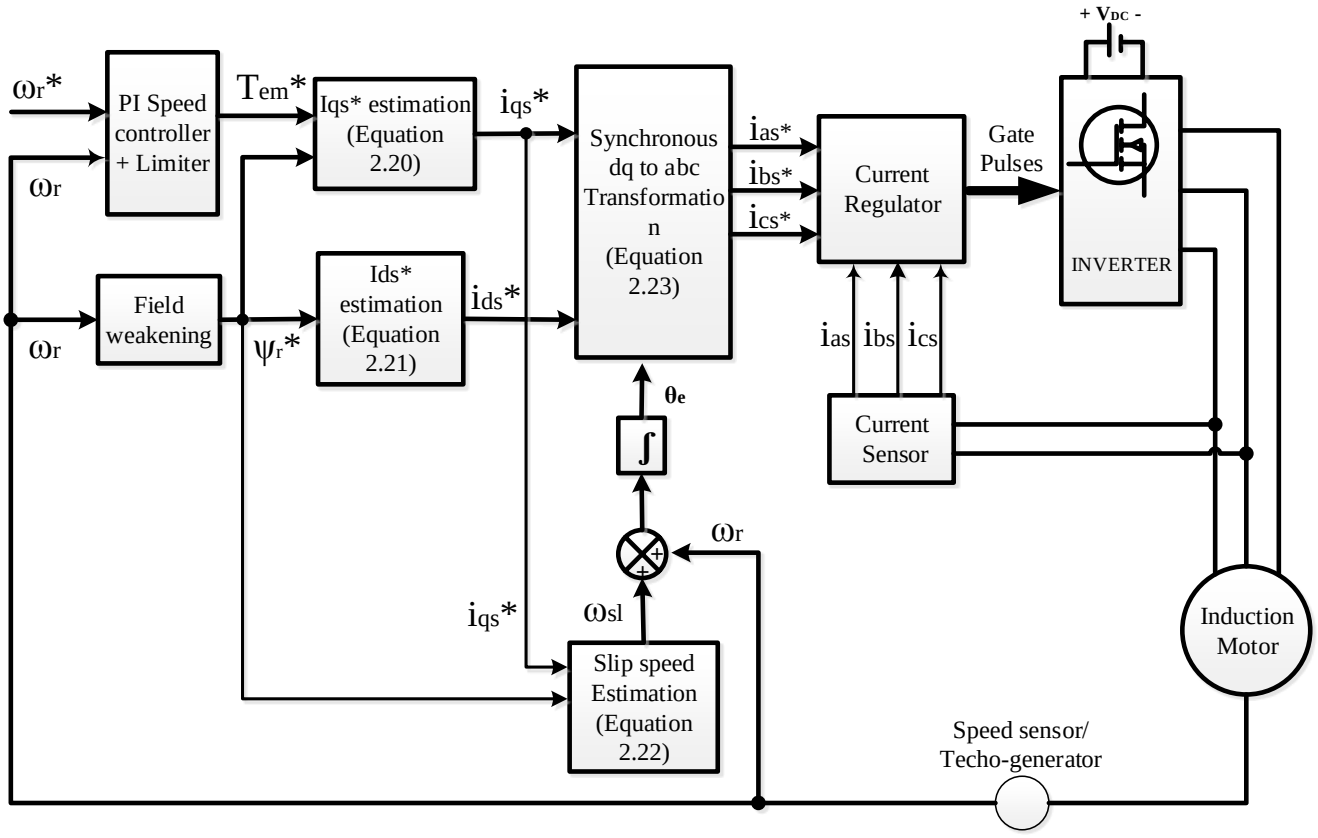

Fig.2.5 Block diagram of Indirect Vector Control of Induction Motor Drive

CHAPTER 3: SIMULATION OF VECTOR CONTROL OF INDUCTION MOTOR

Indirect vector control of induction motor is simulated for 30hp and 2hp induction motor in Matlab/Simulink environment using SPS toolbox in the discrete time frame. Parameters of the machines are tabulated in the Table I in Appendix I.

The Simulink model of indirect vector control is shown in Fig. 3.1 and Fig. 3.2. In this speed controller is used to generate the command torque and the flux weakening block to generate reference flux.

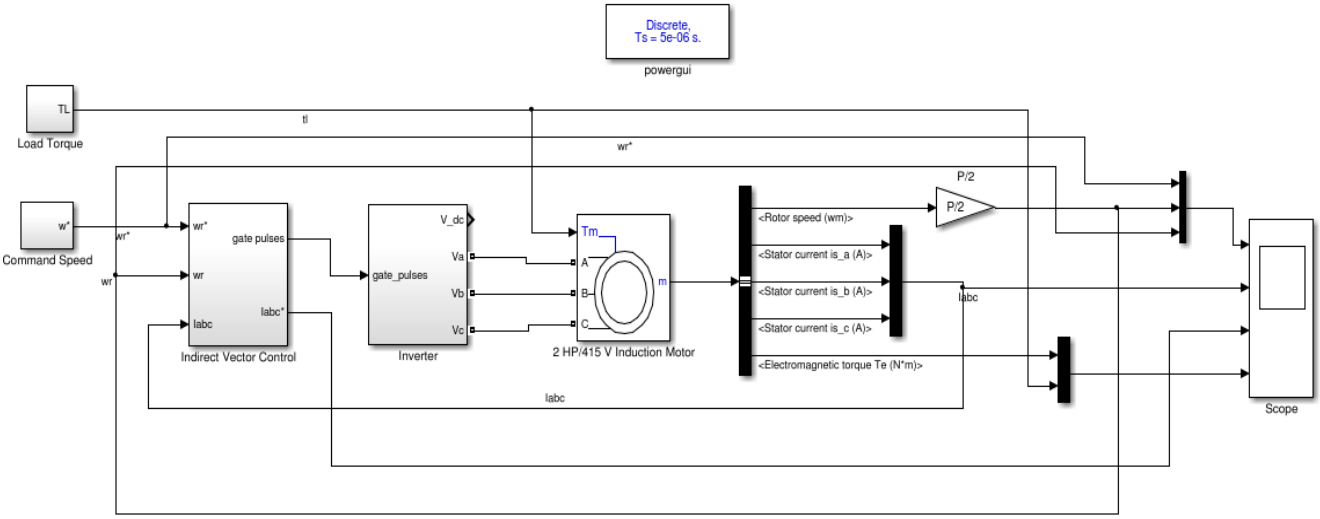

Fig. 3.1 Simulation model of indirect vector control of IM drive

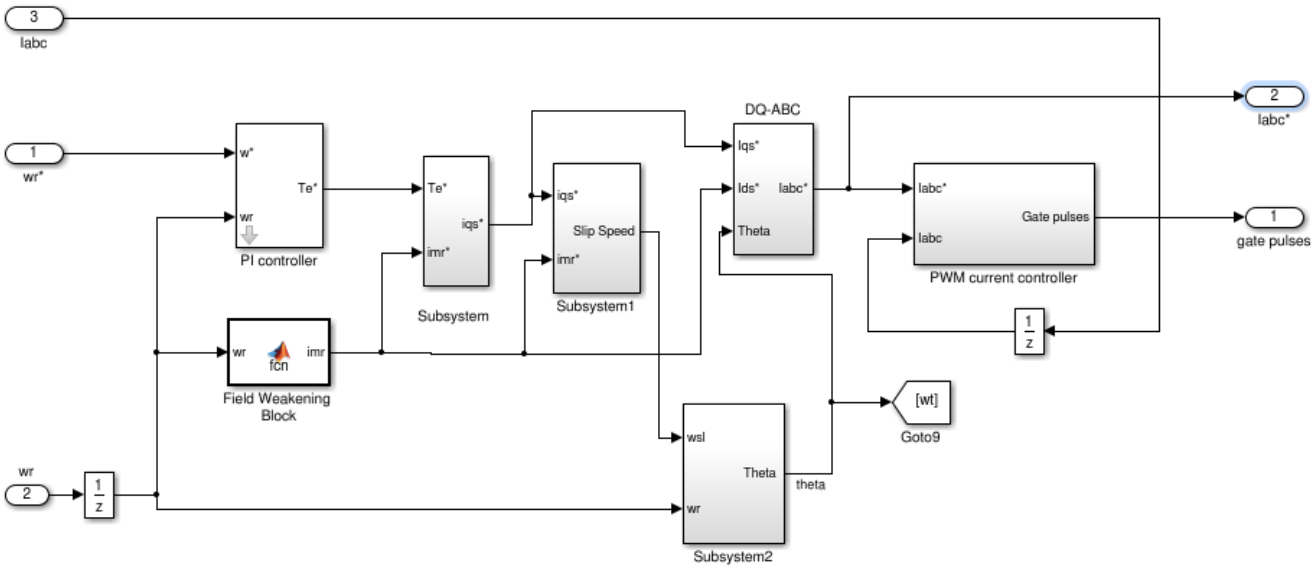

Fig. 3.2 Indirect vector control Block

3.1 SPEED CONTROLLER

The work of speed controller is to generate suitable reference torque signal from the speed error (difference between actual speed and the reference speed). There are many speed controller techniques are available like PI controller, Fuzzy Logic base controller, Intelligent Speed controller (Fuzzy + PI) etc. from all of the above, I have used PI controller to compelete this simulation.

PI controller

In the continuous time frame, the proportional integral controller can be represent as,

$$T_{em} = K_p(\omega_r^* - \omega_r) + K_I \int(\omega_r^* - \omega_r)\, dt \quad (3.1)$$

But we simulate the model in the discreet time frame, so the above equation can be converted in DTF as below:

For the N^{th} sample equation can be written as

$$T_{em\,(N)} = K_p\, \omega_{er(N)} + K_I \sum_{N=1}^{N}\{\omega_{er(N)}\} \quad (3.2)$$

For $(N-1)^{th}$ sample

$$T_{em\,(N-1)} = K_p\, \omega_{er(N-1)} + K_I \sum_{N=1}^{N-1}\{\omega_{er(N-1)}\} \quad (3.3)$$

If the $(N-1)^{th}$ sample pass through limiter, it would become the reference of $(N-1)^{th}$ sample,

$$T^*_{em(N-1)} = K_p\, \omega_{er(N-1)} + K_I \sum_{N=1}^{N-1}\{\omega_{er(N-1)}\} \quad (3.4)$$

By subtracting the equation (3.2) from equation (3.4) we'll get,

$$T_{em\,(N)} = T^*_{em(N-1)} + K_p\, \{\omega_{er(N)} - \omega_{e(N-1)}\} + K_I\, \omega_{er(N)} \quad (3.5)$$

The equation (3.5) shows the basic PI controller in DTF, can be modelled as shown in Fig.3.3. The electromagnetic torque of N^{th} sample will be pass through the Limiter, so that the reference value of torque will in certain liming band.

3.2 FIELD WEAKENING BLOCK

Field weakening (FW) operation is considered when reference speed (ω_r^*) is more than the base speed (ω_{base}). After all the vector control technique make induction motor

operation as dc motor and in dc motor we use Field weakening method to operate it for greater than base speed.

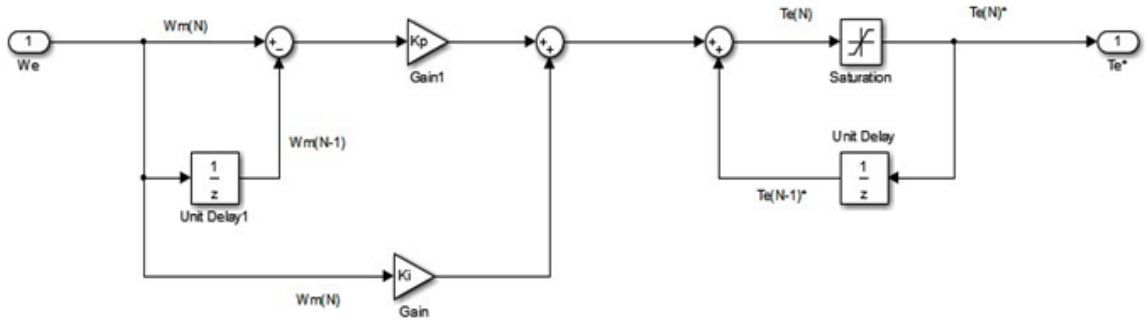

Fig.3.3 Speed controller using PI control logic in MATLAB

Here also the same method has been consider to reduce the flux in proportional to the speed when speed is greater than base speed (ω_{base}).

$$i^*_{mr} = i_m \qquad \text{When} \quad \omega_r < \omega_{base}$$

$$i^*_{mr} = K_f \frac{i_m}{\omega_r} \qquad \text{When} \quad \omega_r \geq \omega_{base}$$

Where i^*_{mr} refers to rms value of magnetizing current, and K_f refers to flux constant.

3.3 i_{qs}* AND i_{ds}* ESTIMATION, SLIP SPEED ESTIMATION AND COORDINATE TRANSFORMATION BLOCK:

Some other blocks in the simulation part like Direct and Quadrature axis (synchronously rotating ref. frame) component of stator current Calculation, Slip speed calculation, Transformation from d^*-q^* current to stationary axis abc-frame component can be easy modelled by equations (2.20), (2.21), (2.22) and (2.23), as shown below Fig.3.4.

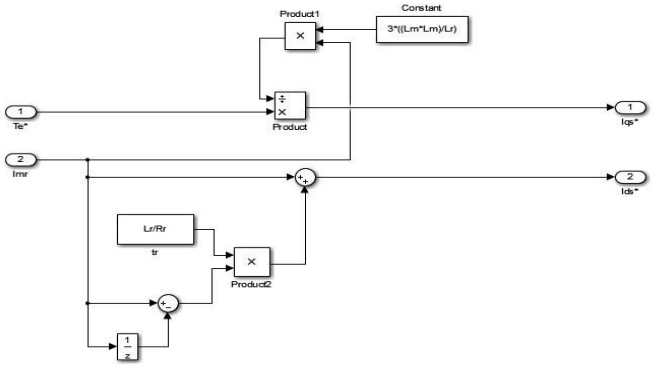

(a)

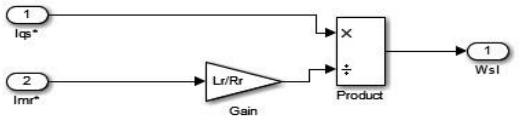

(b)

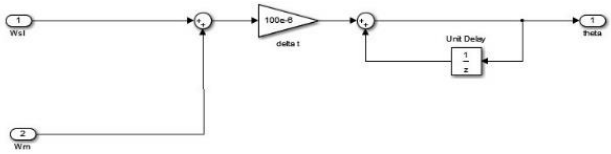

(c)

Fig.3.4 (a) Estimation of iqs and ids*. (b) Estimation of slip speed. (c) Estimation of Θe*

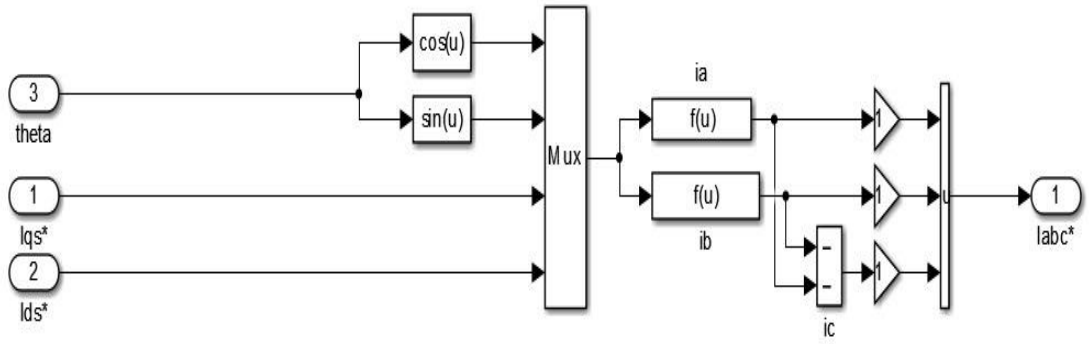

Fig.3.4 (d) Dq to abc coordinate transformation

3.4 SPEED SENSOR

It sense the speed of rotating machine it can either be a speed encoder or Tacho-generator with Voltage sensor. Here, for the hardware purpose I have used the Tacho-generator (mounted on the same shaft with induction motor) with Voltage sensor (which is calibrated in terms of rpm output).

3.5 CURRENT REGULATORS

Diverse current regulating techniques like, Sinusoidal PWM, synchronous dq frame PI regulator, stationary frame PR, stationary frame PI and hysteresis current regulator etc. In all of those regulators Hysteresis Current control method of VSI offers an matchless transient response in contrast with other analog and digital method, which makes it suitable to accept this method in all cases where high accuracy, wide bandwidth, and robustness are essential.

Sinusoidal PWM

Here, depending upon the frequency of carrier, the switching device will operated by comparing the reference current and actual current, the error signal will generate then it will pass through PI controller to give the Modulation Index (MI). MI signal will pass through Limiter then multiply with sine wave having unity peak value, after that it compare with carrier wave to generate Gate Pulse signal. Modelling of this technique is shown in Fig 3.5.

Hysteresis Current Regulator

Hysteresis control technique is fundamentally an analogic technique. In spite of the merits given by digital controllers, in term of flexibility, maintenance integration interfacing, their correctness and response speed are often insufficient for current control in highly

challenging applications, such as active filters and high- precision drives. In these applications, reference current waveform categorized by high harmonic content and fast transient must followed by good accuracy. In these belongings, the hysteresis technique can be a fine solution, provided some improvement are introduced to overcome its main limitations, which are sensitivity to phase commutation interference and switching frequency. The modelling of this technique is shown in Fig. 3.6.

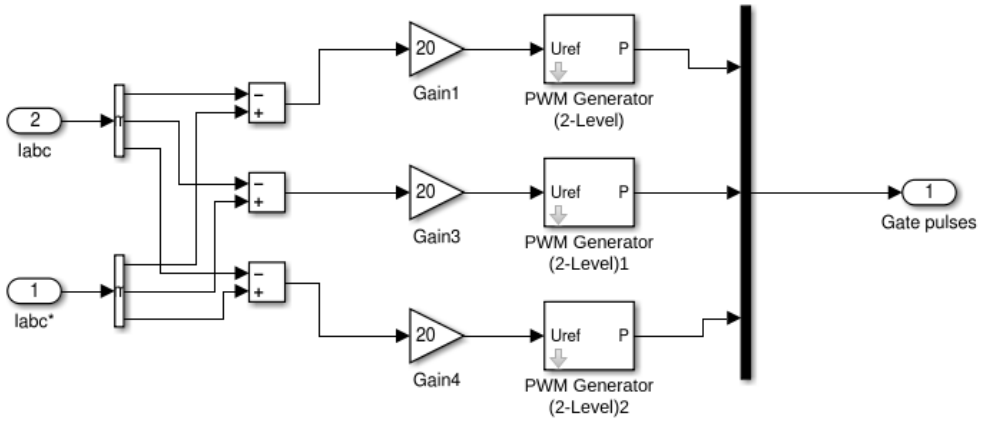

Fig.3.5 Sinusoidal PWM method to generate gate pulse for two level Inverter

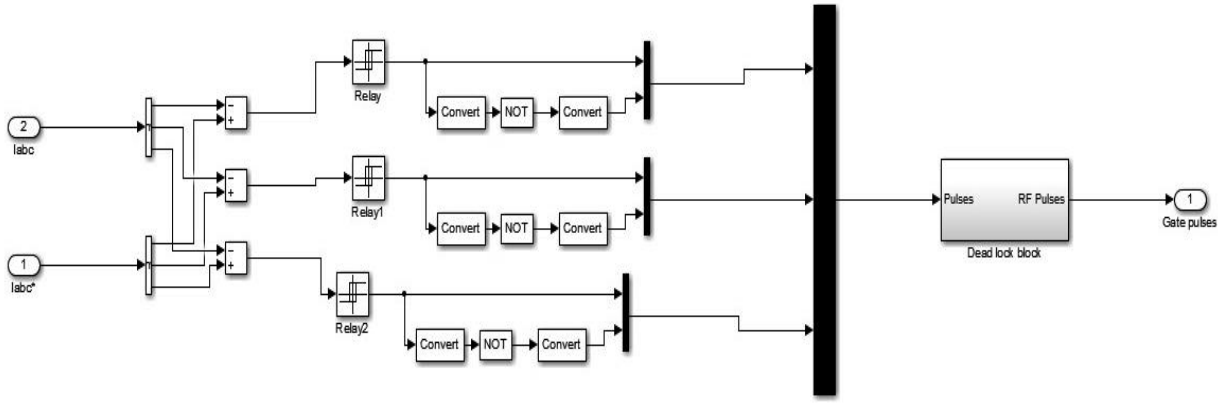

Fig. 3.6 Hysteresis current regulator to generate gate pule for inverter

3.6 SIMULATION RESULTS

Simulation of Indirect Vector Controlled IM drive has been discussed in the previous sections. In this section, the simulation results of those simulations for 30Hp and 2Hp induction motors are discussed and their parameters are listed in Appendix I. The dynamic performance of the indirect vector controlled drive are plotted at different operating conditions such as starting, speed reversal and load perturbation.

3.6.1 Staring Dynamics

Initially the motors are started with a reference speed of 250 electrical rad/s at no-load torque. As the motor is started, a starting torque will be developed to accelerate the machine. Once the motor reaches the reference speed, the torque developed settles at load torque as shown in Fig. 3.7.

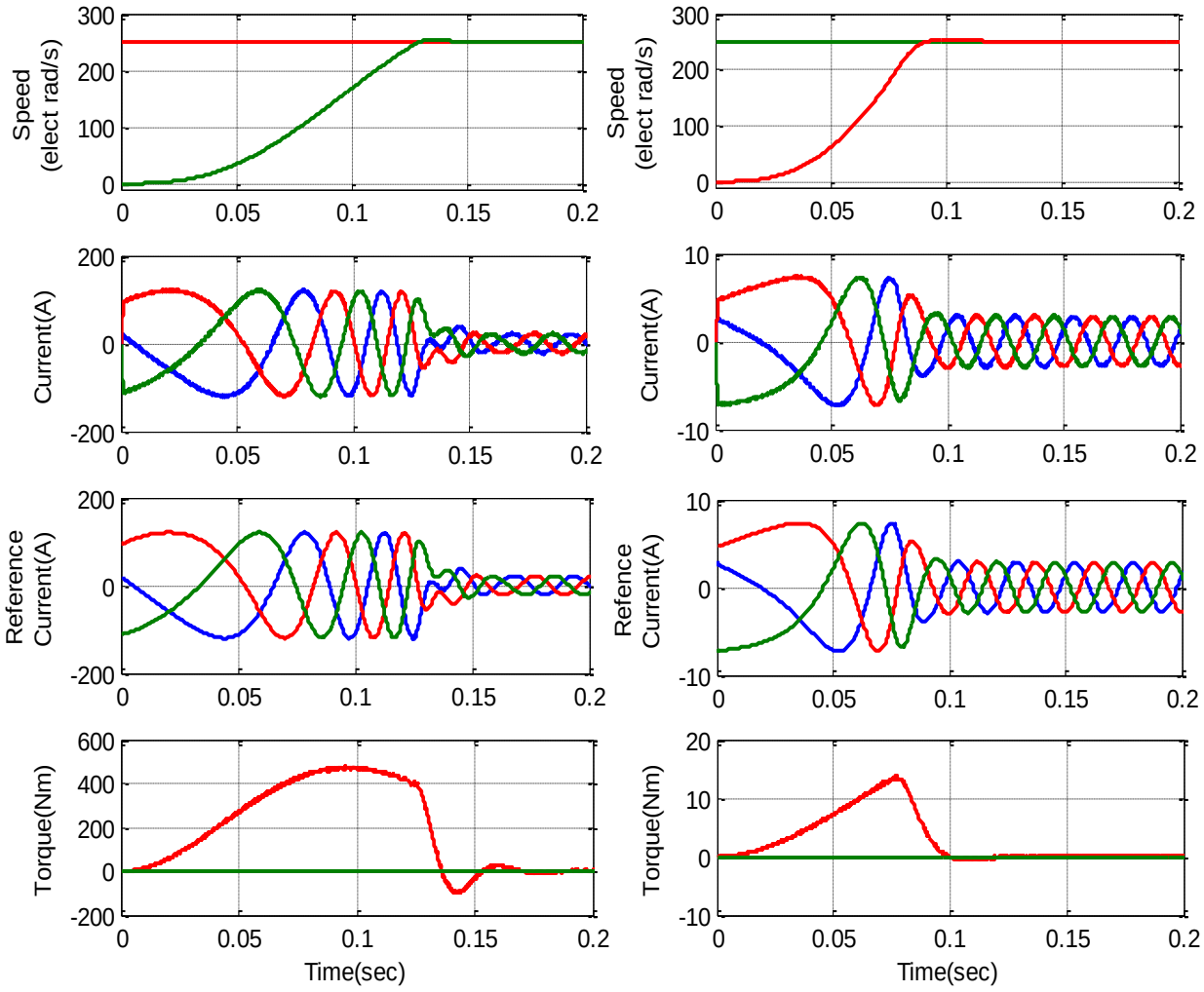

Fig.3.7 Starting Dynamics of 30HP and 2HP induction motor

3.6.2 Speed Reversal Dynamics

When the reference speed change from +250 electrical rad/sec. to -250 electrical rad./sec., the controller initially reduces the frequency of stator currents followed by the phase reversal to get the motor shaft rotation in the reverse direction. As the load conditions are same, so stator current will get settled in the same magnitude as it was before reversal, however the phase sequence will change to get rotating magnetic field in reverse direction as shown in Fig. 3.8.

3.6.3 Load Perturbation Dynamics

This dynamic study is really important as the speed of the motor should not change for any load disturbances. At t=2s, a sudden load torque equal to rated motor torque is applied when it is operating at a speed of 250 electrical rad/sec. Sudden application of load causes an instantaneous drop in speed. In response of this drop, speed controller increases the reference torque (T_{em}^{*}) value. Therefore, the developed electromagnetic torque (T_{em}) of motor drive increases and the motor speed settles at set value with increase in stator winding currents.

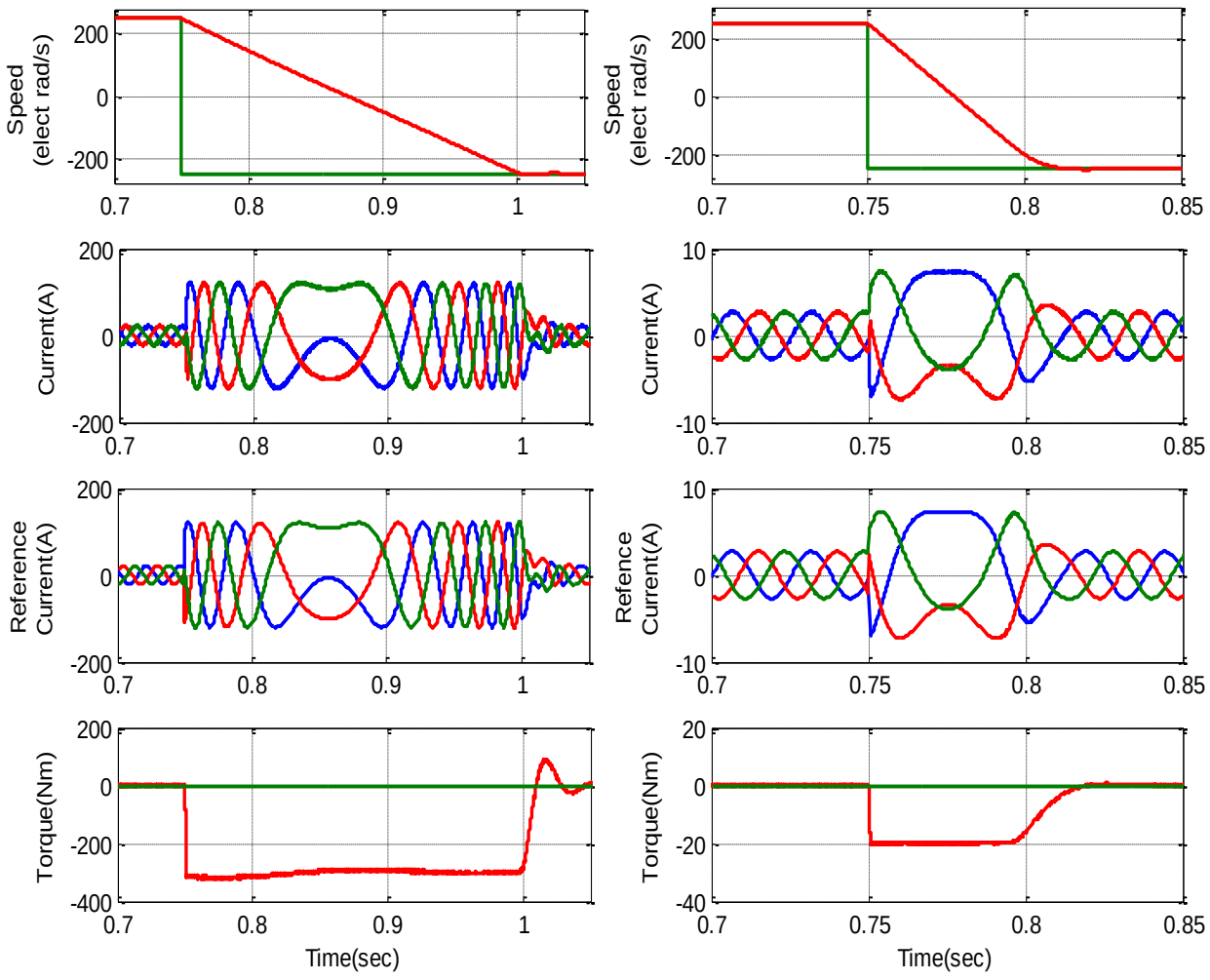

Fig.3.8 Speed Reversal dynamics of 30HP and 2HP induction motor

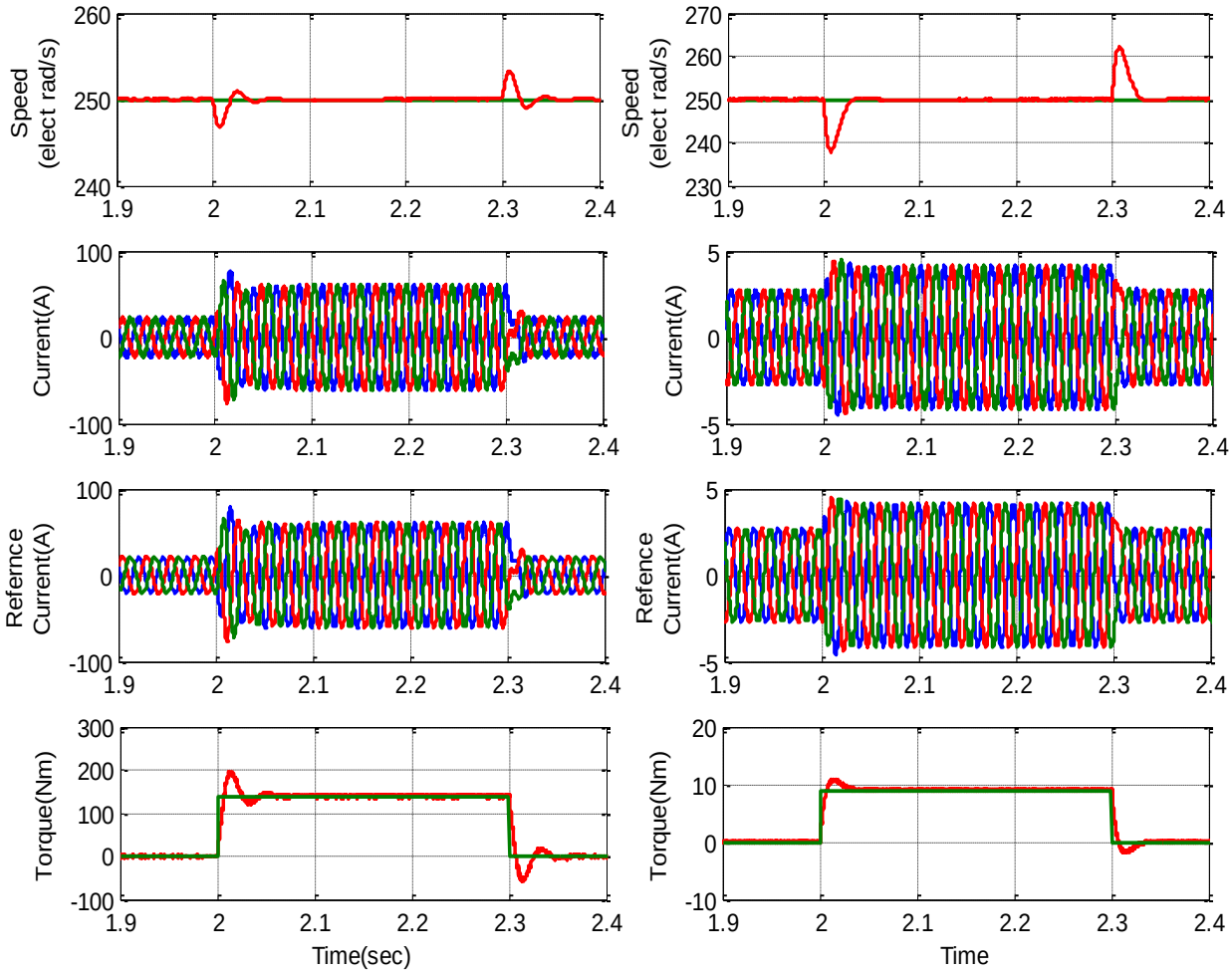

Fig.3.9 Load perturbation dynamics of 30HP and 2HP induction motor

3.7 CONCLUSION

This chapter discusses in brief the principle of vector control and the indirect vector control scheme is derived from the rotor voltage equations in synchronously rotating reference frame. The closed loop performance of the indirect vector control drive is simulated on 2HP and 30HP motors. The detailed results of the simulation are presented in terms of starting performance, speed reversal and load perturbation. We can notice that during each disturbance the controller senses the disturbance and responds adequately by bringing back the controlled variable to its reference value. These results validate the indirect vector control model and the effectiveness of the system modeling and simulation.

CHAPTER 4: SPEED ESTIMATION FOR INDUCTION MOTOR DRIVE

4.1 INTRODUCTION

Indirect vector control of induction motor is widely used in high performance AC drives. To decouple the torque and flux producing components of the stator current and to acquire speed loop feedback, the knowledge of rotor position is required. The speed sensors such as tacho-generators or digital encoders are usually used in vector control for rotor position information. But these speed sensors have some limitations and shortcomings:

- They add to hardware complexity e.g. require motor shaft extension and couplings for their mounting.
- They add to the cost and the size of the drive systems
- Hostile environments limits their application and reliability

These limitations of the speed sensor in the vector control leads to estimating speed in a ‘sensorless’ way by using machine’s terminal voltages and currents which makes them more cheaper and reliable in hostile environments as well. Various speed estimation techniques [25]-[28] have been adopted over the years for sensorless vector control inducton machines. But these various techniques use additional control algorithms and their implementation is compuationally complex. In recent times, the mathematical processing power offered by the digiatl signal processors and FPGAs, have improved the performance of the sensorless vector control motor drive comparable to that of a motor drive using position feedback. Also these high speed multithreaded processors are becoming cheaper with each passing day- in turn decreasing the drive-system cost.

Speed sensorless vector control uses information from intsantaneous stator voltage and currents in comination with machine model to estimate the rotor position as shown in Fig. 4.1. The speed estimation techiques assumes all the machines parameters to be constant, but in reality these machine parameters such as rotor and stator resistances change with temperature, saturation level and frequency. Hence these parameter variations increases the error between the estimated and the actual speed which deteriorates the performance of the drive.

In this chapter the different speed estimation techniques for sensorless vector control of induction machine are discussed and their sensitivity towards stator resistance variation.

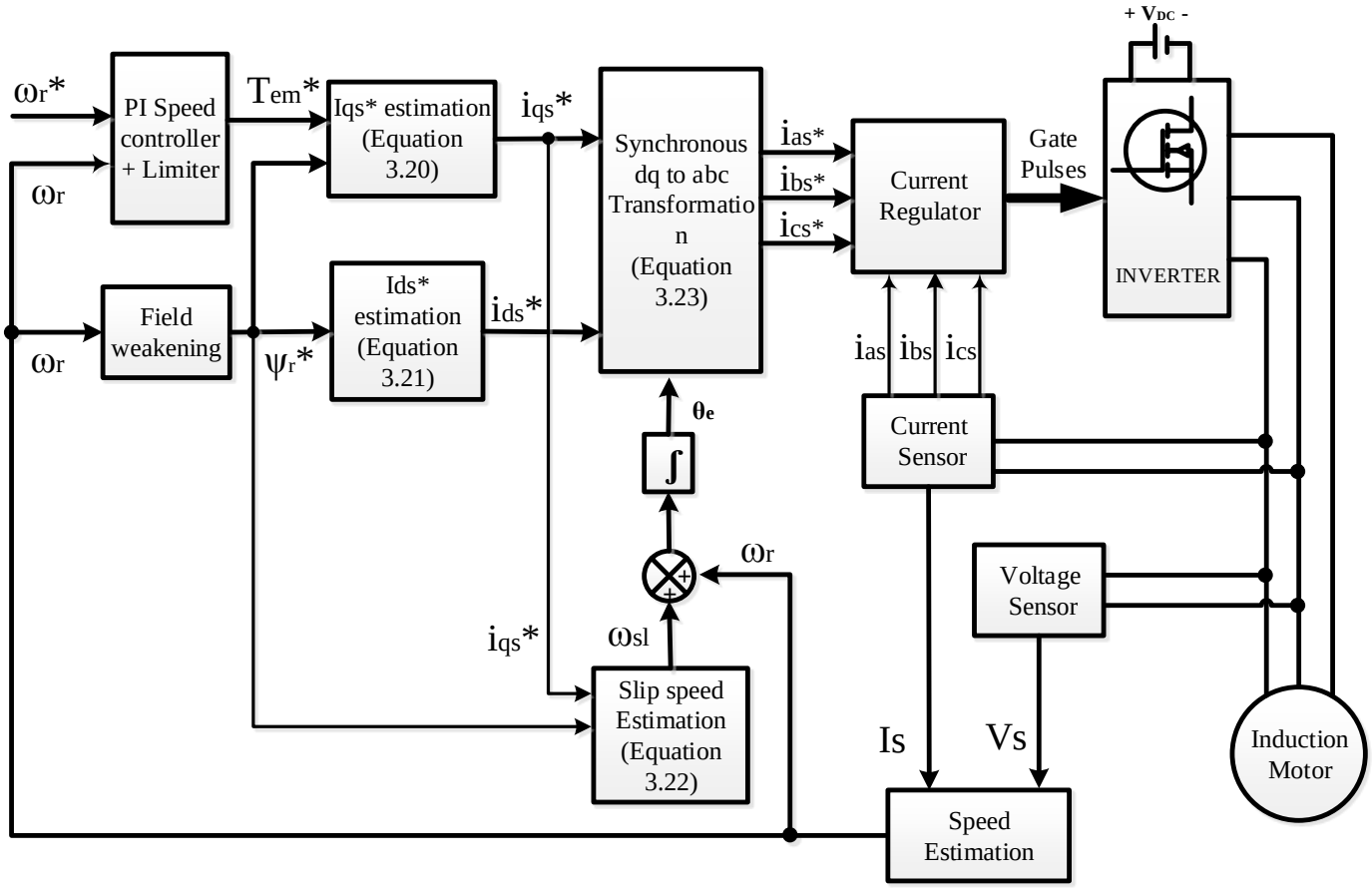

Fig.4.1 Block diagram of Sensorless Vector Control of Induction Motor Drive

In general estimators are categorized into two types: fundamental machine model techniques and saliency based techniques. Fundamental machine models uses the machine dynamic equations, neglect the space harmonics and assume the sinusoidal flux distribution. Saliency based estimation techniques include sliding mode observers, Lueunberger observer, various artificial intelligence techniques, open-loop estimator and model reference adaptive systems. Among these open-loop estimators and MRAS techniques are discussed in detail as these are easier to implement in real time requiring less mathematical computations [30].

4.2 OPEN LOOP ESTIMATORS

In open-loop estimator, the measured stator voltages and currents are used to estimate the flux linkage components from which the speed is estimated. The expression for rotor speed ω_r can be written as:

$$\omega_r = \omega_s - \omega_{sl} \tag{4.1}$$

Where ω_s is the speed of the rotor flux-linkage phasor and ω_{sl} is the angular rotor-slip frequency. The mathematical expression for rotor flux angle θ_s in terms of dq components (Ψ_{rd} and Ψ_{rq}) of rotor flux-linkage phasor is defined as:

$$\theta_s = \tan^{-1}\left(\frac{\Psi_{rq}}{\Psi_{rd}}\right) \tag{4.2}$$

Therefore,

$$\omega_s = \frac{d\theta_s}{dt} = \frac{d}{dt}\left[\tan^{-1}\left(\frac{\Psi_{rq}}{\Psi_{rd}}\right)\right] = \frac{\Psi_{rd}\,\frac{d\Psi_{rq}}{dt} - \Psi_{rq}\,\frac{d\Psi_{rd}}{dt}}{{\Psi_{rd}}^2 + {\Psi_{rq}}^2} \tag{4.3}$$

The rotor voltage equations of the induction machine expressed in rotor flux oriented frame are given as:

$$V_{dr}^* = 0 = R_r\, i_{rd} + p\,\Psi_{rd} - \omega_{sl}\,\Psi_{rq} \tag{4.4}$$

$$V_{qr}^* = 0 = R_r\, i_{rq} + p\,\Psi_{rq} + \omega_{sl}\,\Psi_{rd} \tag{4.5}$$

Where

$$\Psi_{rd} = L_r\, i_{rd} + L_m\, i_{sd} \tag{4.6}$$

$$\Psi_{rq} = L_r\, i_{rq} + L_m\, i_{sq} \tag{4.7}$$

Substituting i_{rd} and i_{rq} from (4.6) and (4.7) into (4.4) and (4.5) yields:

$$\omega_{sl}\,\Psi_{rq} = p\,\Psi_{rd} + \frac{R_r}{L_r}\left[\Psi_{rd} - L_m\, i_{sd}\right] \tag{4.8}$$

$$-\omega_{sl}\,\Psi_{rd} = p\,\Psi_{rq} + \frac{R_r}{L_r}\left[\Psi_{rq} - L_m\, i_{sq}\right] \tag{4.9}$$

Multiplying (4.8) by Ψ_{rq} and (4.9) by Ψ_{rd} and then subtracting them yields:

$$\omega_{sl} = \frac{L_m}{T_r\,|\Psi_r|^2}\left(\Psi_{rd} i_{sq} - \Psi_{rq} i_{sd}\right) \tag{4.10}$$

Finally we obtain the rotor speed from (4.1), (4.3) and (4.10) as:

$$\omega_r = \frac{\Psi_{rd}\,\frac{d\Psi_{rq}}{dt} - \Psi_{rq}\,\frac{d\Psi_{rd}}{dt}}{|\Psi_r|^2} - \frac{L_m}{T_r\,|\Psi_r|^2}\left(\Psi_{rd} i_{sq} - \Psi_{rq} i_{sd}\right) \tag{4.11}$$

Where $T_r = \frac{L_r}{R_r}$ and $\Psi_r = \sqrt{{\Psi_{rd}}^2 + {\Psi_{rq}}^2}$ is the rotor flux phasor. The rotor flux linkage components are first deduced from the stator voltage equations as given below:

$$\frac{L_m}{L_r}\frac{d}{dt}\Psi_{rd} = V_{sd} - R_s\, i_{sd} + L_s\left(1 - \frac{{L_m}^2}{L_r L_s}\right)\frac{d}{dt}\, i_{sd} \tag{4.12}$$

$$\frac{L_m}{L_r}\frac{d}{dt}\Psi_{rd} = V_{sd} - R_s\, i_{sd} + L_s\left(1 - \frac{{L_m}^2}{L_r L_s}\right)\frac{d}{dt}\, i_{sd} \tag{4.13}$$

First the rotor flux linkage components from (4.12) and (4.13) are used in (4.11) to extract the rotor speed. The implementation of the open loop estimator is shown in Fig. 4.2.

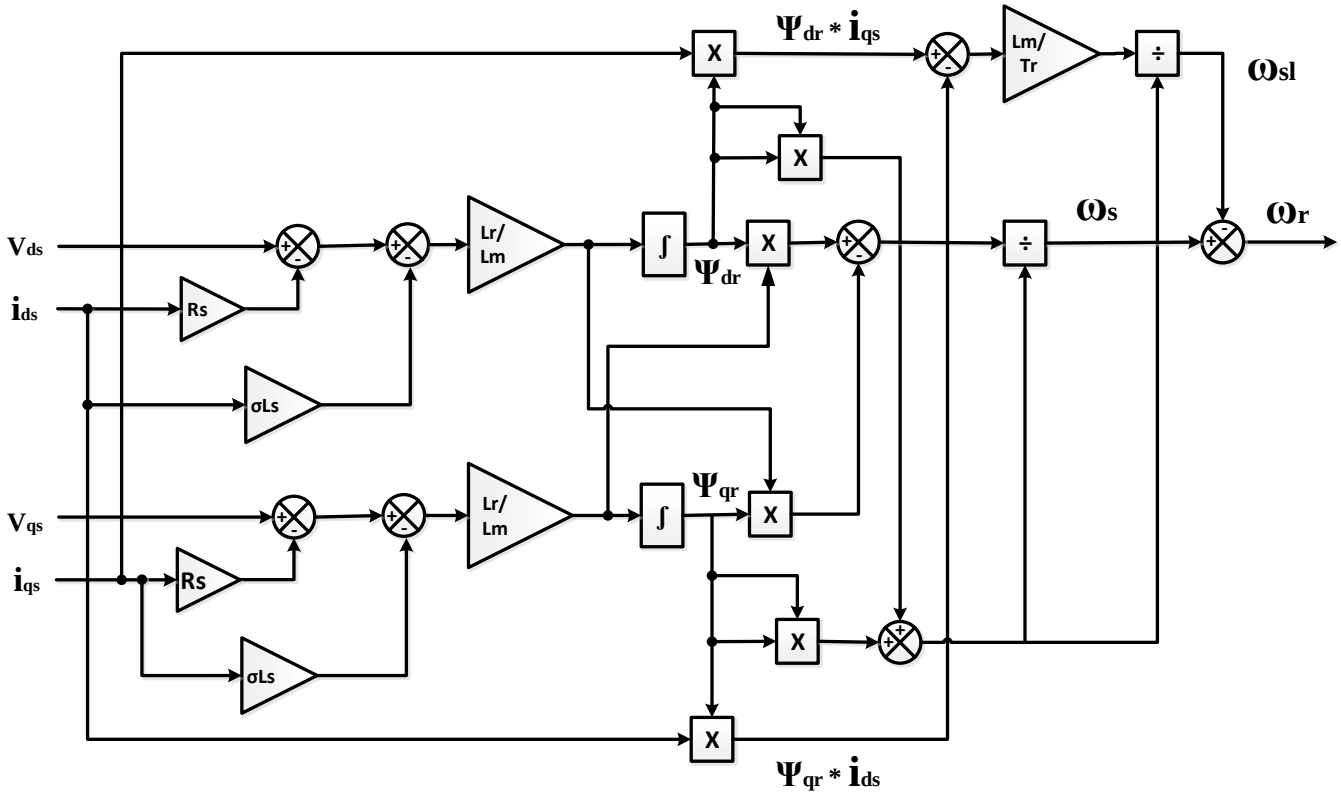

Fig.4.2 Block diagram of Open-loop speed estimator

In open loop estimators, the parameter variations have significant influence on the performance of the drive both in transient and steady states [29]. The accuracy is poor at low speeds and the drive may suffer from instability problem. But in comparison the closed loop estimators are more robust to parameter changes and noise. The following sections reviews the basic MRAS structure and different MRAS based speed estimation techniques.

4.3 MODEL REFERENCE ADAPTIVE SYSTEM

"An adaptive system is a system where in addition to the basic feedback structure, additional measures (such as adjustment of controller parameters or generation of extra input signals) are taken to compensate for variations in the process dynamics or for variations in the disturbances, in order maintain an optimal performance of the system".

Model reference adaptive systems (MRAS) belongs to the class of direct adaptive systems where, unlike indirect adaptive systems, no explicit identification of the process can be recognized. Among different types of adaptive system strategies, MRAS has attracted much attention because of their simplicity and direct physical interpretation. The high performance ability and easy implementation in real-time has made MRAS one of the major approaches in adaptive control and estimation. The commonly applied MRAS structure uses a parallel reference model also known as parallel MRAS as shown in Fig. 4.3. In this structure either the difference between the process output and the reference output or the difference between the states of the process and of the reference model are minimized by adjusting controller gains K_a and K_b. The advantage of the parallel MRAS structure is that it allows excellent noise-rejection which is helpful in unbiased estimates. A basic structure of MRAS is shown in Fig. 4.4 where X represents the state variable of the system. The reference model is based on a set of equations which does not include the parameter to be estimated. On the contrary, the adaptive model is used to observe the same state variables with different sets of equations employing different inputs which include the parameter to be estimated. The stability of a drive system is achieved by minimizing the error ε between the signals using a set of adaptive laws. As the error between adjustable and reference model diminishes, the estimated parameter $\hat{Y}$ converges to its true value Y. In general, any MRAS 'reference model' represents the demanded dynamics of the actual system and the 'adjustable model' represents the same structure as the reference, but one with adjustable parameters to the converge the system to the demanded dynamics.

In the speed estimation using MRAS, the reference model is derived from set of equations of induction motor model (usually voltage model) that does not involve rotor speed and the adjustable model is based on set of equations (usually motor current model) where the rotor speed is involved. The output of the two models are usually the induction machine's state variables such as the rotor flux, back e.m.f or reactive power. The MRAS scheme makes use of the redundancy of two-machine models of different structures that estimate the same

state variables. Both models are referred to in the stationary reference frame. The difference between the outputs of the reference and the adaptive models forms the error function which is then used to drive an adaptation mechanism which generates the estimated speed. Depending upon the state variables they estimate, MRAS observers can be classified as:

1. Rotor Flux based MRAS,
2. Back e.m.f basd MRAS,
3. Reactive power based MRAS.

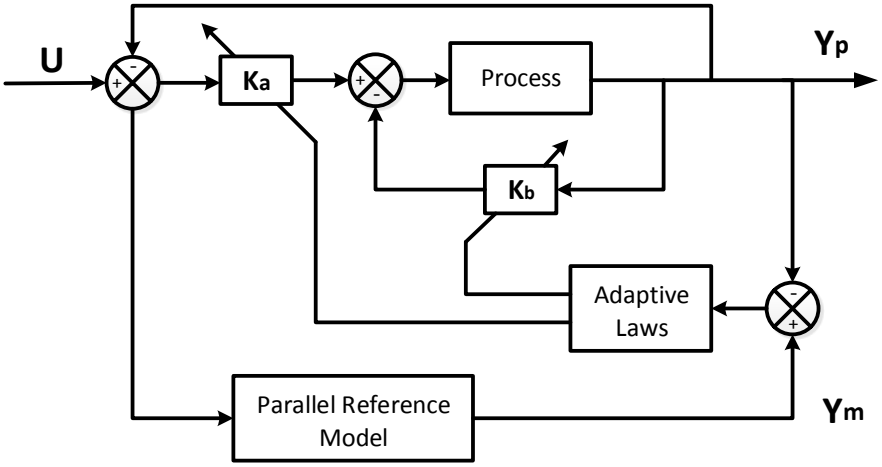

Fig.4.3 MRAS structure with a parallel reference model

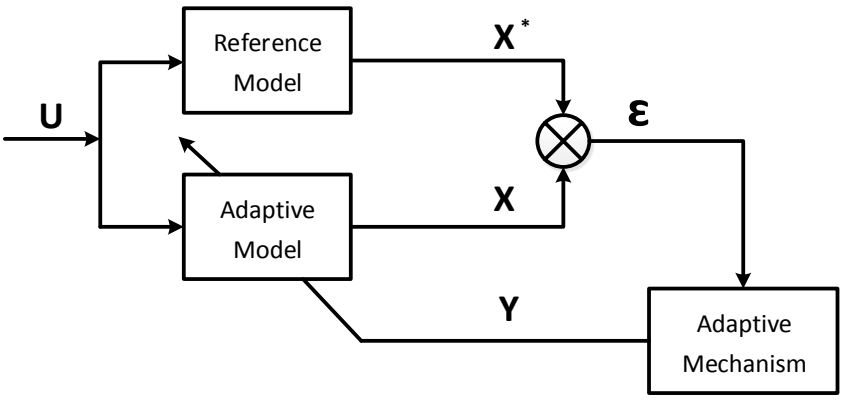

Fig.4.4 Basic MRAS structure

4.3.1 ROTOR FLUX BASED MRAS

Rotor flux based MRAS for IM drives was first proposed by Tamai et al. [43, 44] in 1985. The basic structure of rotor flux based MRAS shown in Fig. 4.5, consists of a reference

model, adaptive model and an adaptation scheme which generates the estimated speed. In the reference model, the rotor flux ($\overline{\Psi}_r$) is calculated from the voltage model in the stationary reference frame and it represents the stator equations of the induction machine. In adaptive model, the rotor flux ($\widehat{\Psi}_r$) is calculated from the current model in the stationary reference frame and it contains stator current components and the rotor speed. The error (ε_r) between these rotor flux signals (state variables) is then used for the estimation of rotor speed ($\widehat{\omega}_r$) by tuning an adaptation scheme.

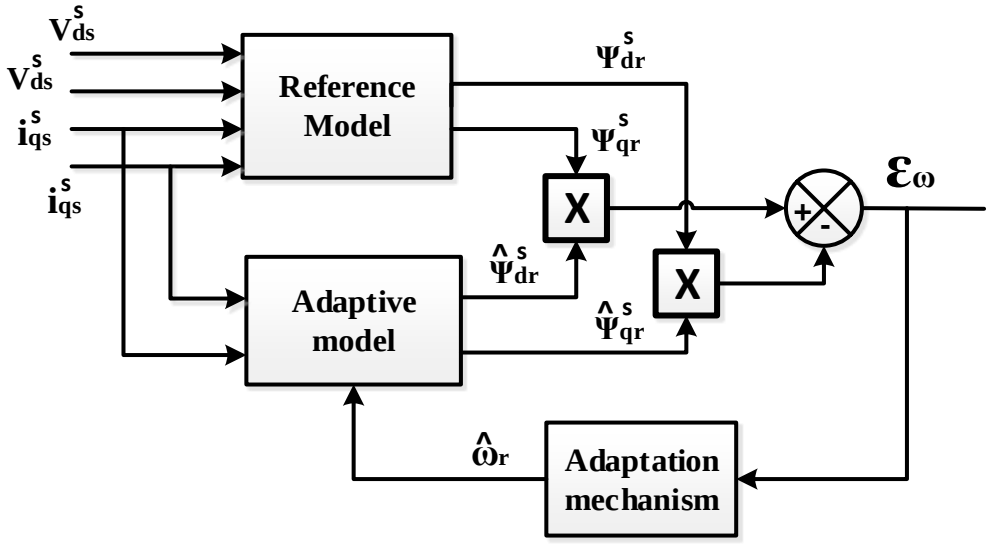

Fig. 4.5 Rotor flux based MRAS speed estimation scheme

Design of rotor flux based MRAS:

The design of rotor flux based MRAS for speed estimation of induction machine is derived using its *dq* model. The stator and rotor voltage equations of the induction machine in the stator reference frame are:

$$V_{ds}^s = R_s\, i_{ds}^s + p\, \Psi_{ds}^s \tag{4.14}$$

$$V_{qs}^s = R_s\, i_{qs}^s + p\, \Psi_{qs}^s \tag{4.15}$$

$$V_{dr}^s = 0 = R_r\, i_{dr}^s + p\, \Psi_{dr}^s - \omega_r\, \Psi_{qr}^s \tag{4.16}$$

$$V_{qr}^s = 0 = R_r\, i_{qr}^s + p\, \Psi_{qr}^s + \omega_r\, \Psi_{dr}^s \tag{4.17}$$

Where,

$$\Psi_{ds}^s = L_s\, i_{ds}^s + L_m\, i_{dr}^s \tag{4.18}$$

$$\Psi_{qs}^{s} = L_s\, i_{qs}^{s} + L_m\, i_{qr}^{s} \tag{4.19}$$

$$\Psi_{dr}^{s} = L_r\, i_{dr}^{s} + L_m\, i_{ds}^{s} \tag{4.20}$$

$$\Psi_{qr}^{s} = L_r\, i_{qr}^{s} + L_m\, i_{qs}^{s} \tag{4.21}$$

Substituting the values of i_{dr}^{s} and i_{qr}^{s} from (4.20) and (4.21) into (4.18) and (4.19) respectively yields:

$$\Psi_{ds}^{s} = L_s\, i_{ds}^{s} + \frac{L_m}{L_r}\left[\Psi_{dr}^{s} - L_m\, i_{ds}^{s}\right] \tag{4.22}$$

$$\Psi_{qs}^{s} = L_s\, i_{qs}^{s} + \frac{L_m}{L_r}\left[\Psi_{qr}^{s} - L_m\, i_{qs}^{s}\right] \tag{4.23}$$

Substituting these values of Ψ_{ds}^{s} and Ψ_{qs}^{s} in stator voltage equations (4.14) and (4.15) yields:

$$V_{ds}^{s} = R_s\, i_{ds}^{s} + p\left(L_s\, i_{ds}^{s} + \frac{L_m}{L_r}\left[\Psi_{dr}^{s} - L_m\, i_{ds}^{s}\right]\right) \tag{4.24}$$

$$V_{qs}^{s} = R_s\, i_{qs}^{s} + p\left(L_s\, i_{qs}^{s} + \frac{L_m}{L_r}\left[\Psi_{qr}^{s} - L_m\, i_{qs}^{s}\right]\right) \tag{4.25}$$

Rearranging (4.24) and (4.25) yields the d-axis and q-axis rotor flux linkages of the reference model as:

$$p\Psi_{dr}^{s} = \frac{L_r}{L_m}\left[V_{ds}^{s} - R_s\, i_{ds}^{s} - \sigma\, pL_s i_{ds}^{s}\right] \tag{4.26}$$

$$p\Psi_{qr}^{s} = \frac{L_r}{L_m}\left[V_{qs}^{s} - R_s\, i_{qs}^{s} - \sigma\, pL_s i_{qs}^{s}\right] \tag{4.27}$$

where $\sigma = 1 - \frac{L_m{}^2}{L_s L_r}$

The *dq* axes rotor flux components for adaptive model are obtained from rotor voltage equations. From (4.20) and (4.21)

$$i_{dr}^{s} = \frac{1}{L_r}\left(\Psi_{dr}^{s} - L_m\, i_{ds}^{s}\right) \tag{4.28}$$

$$i_{qr}^{s} = \frac{1}{L_r}\left(\Psi_{qr}^{s} - L_m\, i_{qs}^{s}\right) \tag{4.29}$$

Substituting the values of i_{dr}^{s} and i_{qr}^{s} from (4.28) and (4.29) into (4.16) and (4.17) respectively yields:

$$p\,\Psi_{dr}^{s} = -\frac{R_r}{L_r}(\Psi_{dr}^{s} - L_m\, i_{ds}^{s}) - \omega_r\,\Psi_{qr}^{s} \tag{4.30}$$

$$p\,\Psi_{qr}^{s} = -\frac{R_r}{L_r}(\Psi_{qr}^{s} - L_m\, i_{qs}^{s}) + \omega_r\,\Psi_{dr}^{s} \tag{4.31}$$

Rearranging (4.24) and (4.25) yields the d-axis and q-axis rotor flux linkages of the adaptive model as:

$$p\,\hat{\Psi}_{dr}^{s} = \frac{L_m}{T_r}\, i_{ds}^{s} - \frac{1}{T_r}\hat{\Psi}_{dr}^{s} - \hat{\omega}_r\hat{\Psi}_{qr}^{s} \tag{4.32}$$

$$p\,\hat{\Psi}_{qr}^{s} = \frac{L_m}{T_r}\, i_{qs}^{s} - \frac{1}{T_r}\hat{\Psi}_{qr}^{s} + \hat{\omega}_r\hat{\Psi}_{dr}^{s} \tag{4.33}$$

where $T_r = \frac{L_r}{R_r}$

Estimated speed is obtained by minimizing the error between the reference model and the adaptive model's flux signals by tuning the adaptation scheme. The practical synthesis technique for MRAS structures which is based on the concept of hyper-stability can be used to design the adaptation mechanism. These rules will ensure that the state error equations of the MRAS structures are globally asymptotically stable. Therefore, the expression for speed tuning signal and estimated speed is given by:

$$\varepsilon_\omega = \Psi_{qr}^{s}\hat{\Psi}_{dr}^{s} - \Psi_{dr}^{s}\hat{\Psi}_{qr}^{s} \tag{4.34}$$

$$\hat{\omega}_r = \left(K_{p\omega} + \frac{K_{i\omega}}{p}\right)\varepsilon_\omega \tag{4.35}$$

The full notation block diagram of rotor flux based MRAS speed estimation scheme is shown in the Fig.4.6. Although the proposed method of rotor-flux-based MRAS speed estimator is simple, but the proposed estimator suffers from motor-parameter variations (especially stator resistance), inaccuracy at low-speed because of poor signal-to-noise ratio, increased inverter non-linearity and flux pure-integration problems which may cause DC drift and initial condition problems. These problems affects the drive's performance at low speeds.

4.3.2 BACK-EMF BASED MRAS

The back e.m.f based MRAS scheme [38, 39] was proposed to provide an improvement over the rotor flux based MRAS scheme. The basic bock diagram of back e.m.f based MRAS is shown in Fig. 4.7. The advantage of the back e.m.f. based MRAS scheme is

that it does not require any pure integration in its reference and adaptive models. Instead of using the rotor fluxes in reference and adaptive models, the back EMF (counter electromotive force) is estimated and compared with the measured quantity to produce a speed error correction signal.

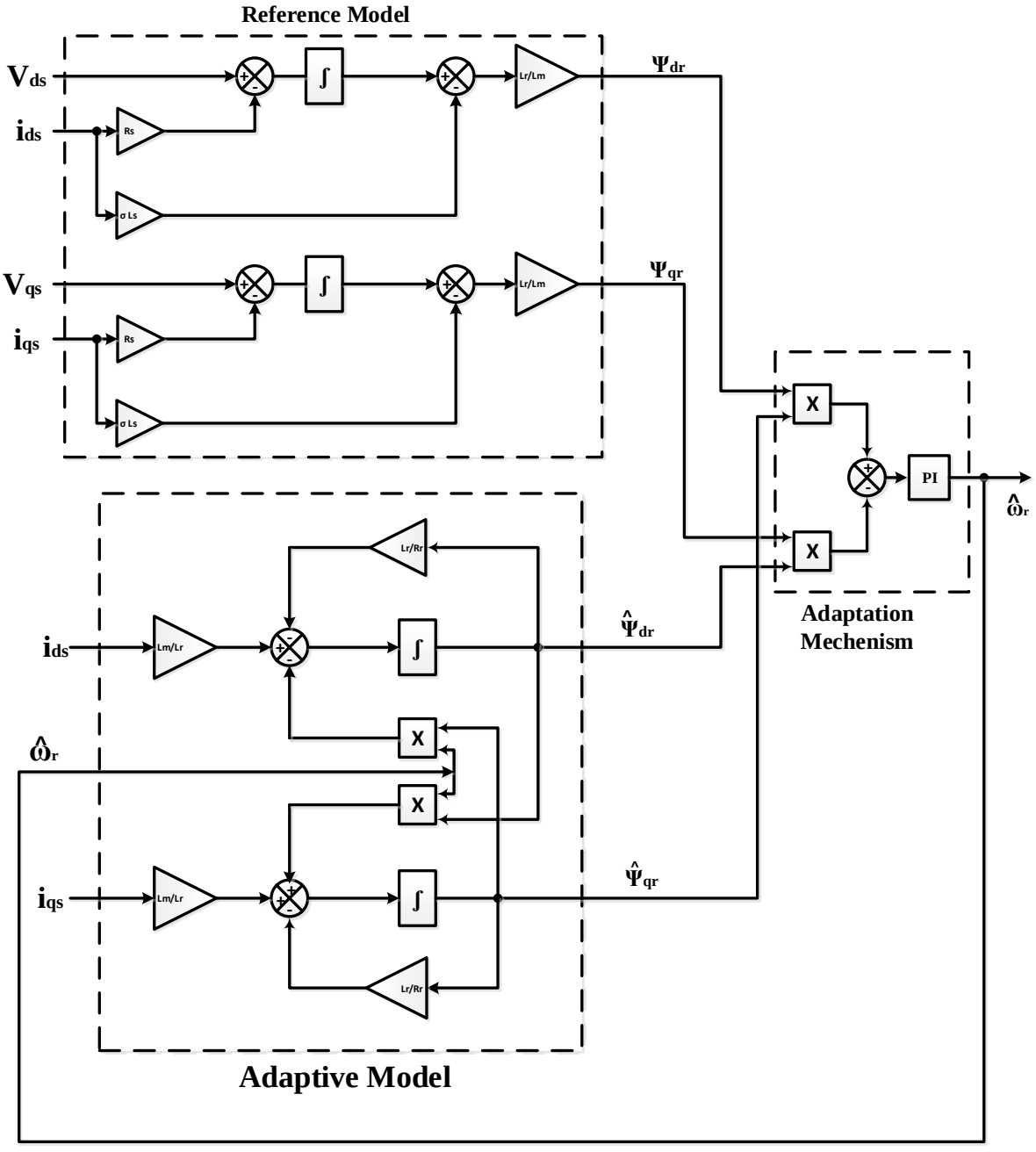

Fig.4.6 Block diagram for Rotor Flux based MRAS speed estimation technique

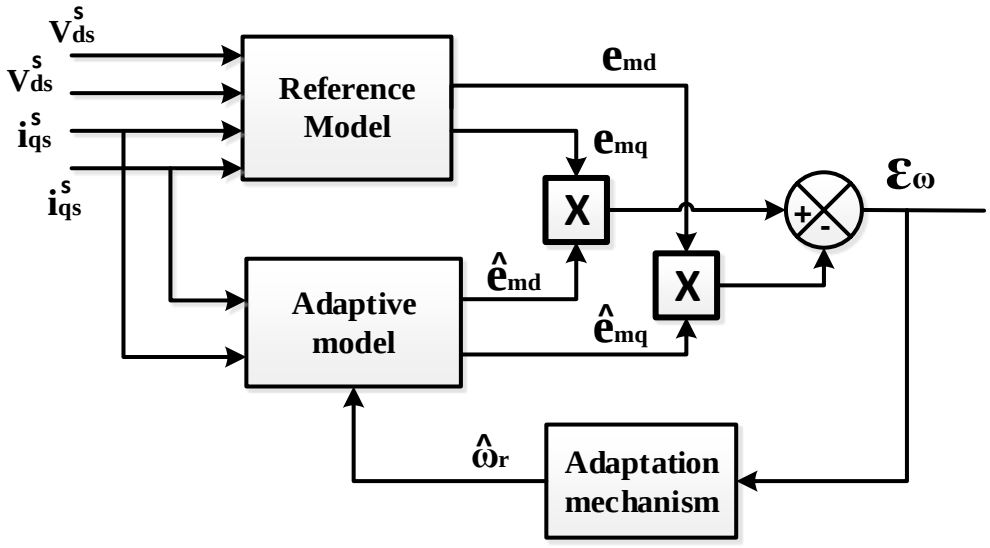

Fig. 4.7 Back e.m.f based MRAS speed estimation scheme

The reference model equations for estimation of back e.m.f are:

$$e_{md} = V_{ds}^{s} - (R_s + L_s p)\, i_{ds}^{s} \tag{4.36}$$

$$e_{mq} = V_{qs}^{s} - (R_s + L_s p)\, i_{qs}^{s} \tag{4.37}$$

The adaptive model equations for estimation of back e.m.f are:

$$e_{md} = \frac{L_m{}^2}{L_r}\left(-\hat{\omega}_r i_{mq} - \frac{1}{T_r} i_{md} + \frac{1}{T_r} i_{ds}\right) \tag{4.38}$$

$$e_{mq} = \frac{L_m{}^2}{L_r}\left(-\hat{\omega}_r i_{md} - \frac{1}{T_r} i_{mq} + \frac{1}{T_r} i_{qs}\right) \tag{4.39}$$

Where

$$p\, i_{md} = -\hat{\omega}_r i_{mq} - \frac{1}{T_r} i_{md} + \frac{1}{T_r} i_{ds} \tag{4.40}$$

$$p\, i_{mq} = -\hat{\omega}_r i_{md} - \frac{1}{T_r} i_{mq} + \frac{1}{T_r} i_{qs} \tag{4.41}$$

Similar to rotor flux based the adaptation scheme for back e.m.f MRAS scheme can be derived as follows:

$$\hat{\omega}_r = \left(K_{p\omega} + \frac{K_{i\omega}}{p}\right) \varepsilon_{\omega} \tag{4.42}$$

Where

$$\varepsilon_\omega = (e_m \otimes \hat{e}_m)$$

$$e_m = e_{md} + j e_{mq} \tag{4.43}$$

$$\hat{e}_m = \hat{e}_{md} + j \hat{e}_{mq}$$

$$\varepsilon_\omega = (e_m \otimes \hat{e}_m) = e_{md}\hat{e}_{mq} - e_{mq}\hat{e}_{md}$$

This MRAS scheme avoids using an integrator in the reference model and hence it does not suffers from drift or initial conditions problems. However, the reference model is sensitive to stator resistance variation but comparatively less sensitive than rotor flux based MRAS. The drive may have stability problems at low stator frequency and also shows less noise immunity due to stator current differentiation. If a current-regulated voltage-source inverter is used in the experimental systems, $i_s = i_s^*$, the i_s can be replaced with i_s^* to avoid noise problem of differentiation.

4.3.3 REACTIVE POWER BASED MRAS

The reactive power based MRAS scheme is shown in Fig. 4.8. Reactive power based MRAS [40, 41] is proposed to estimate the rotor speed eliminating the stator resistance sensitivity completely. As the stator resistance varies with the temperature, its variation affects the performance and stability of the rotor flux and back e.m.f based MRAS speed estimators, especially at low speeds.

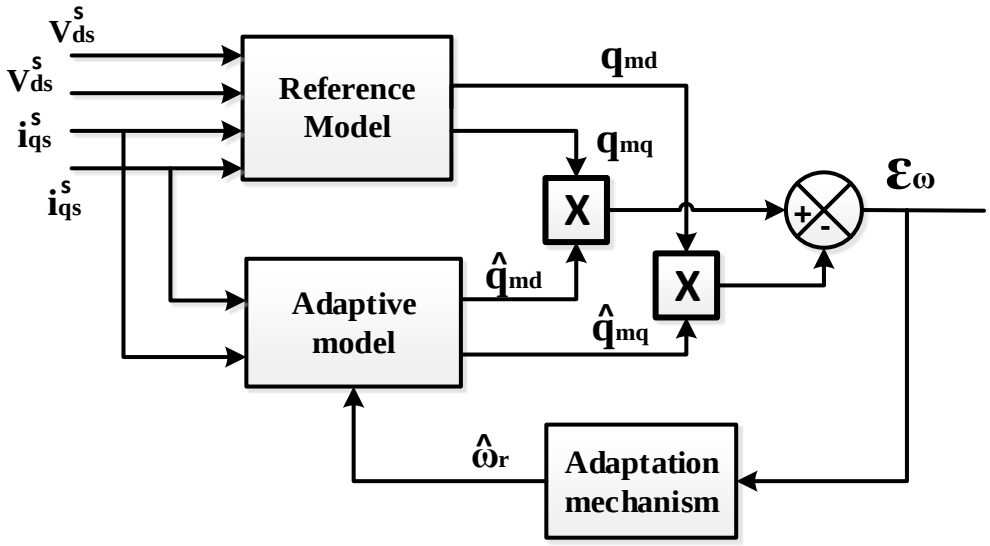

Fig. 4.8 Reactive power based MRAS speed estimation scheme

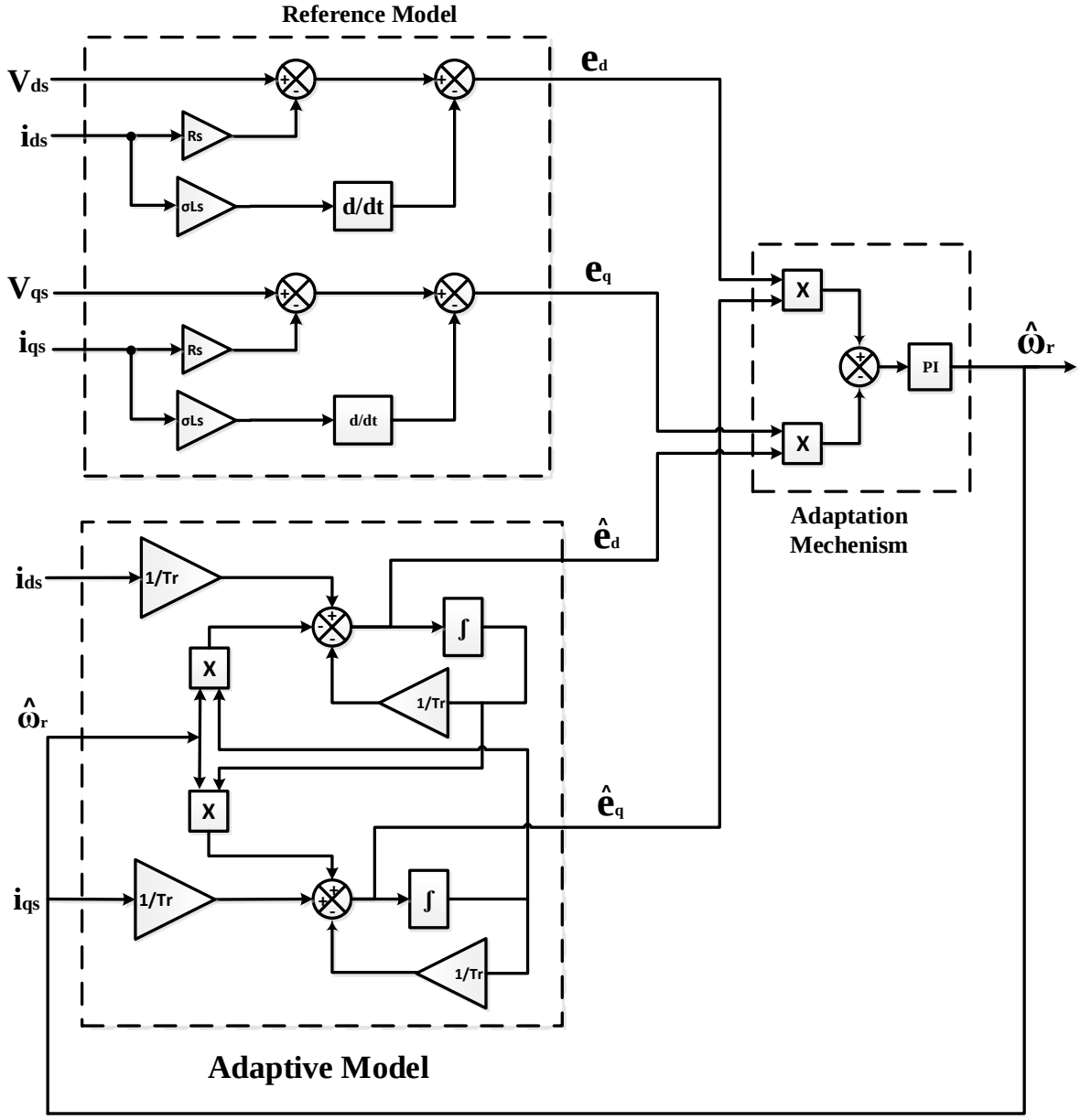

Fig.4.9 Block diagram for Back-emf based MRAS speed estimation technique

The instantaneous reactive power maintaining the magnetizing current can be expressed as:

$$q_{ref} = i_s \otimes e_m \tag{4.44}$$

Substituting (4.36) and (4.37) for e_m in (4.44) yields the reactive power for reference model:

$$q_{ref} = V_{sq} i_{sd} - V_{sd} i_{sq} \tag{4.45}$$

While in the adaptive model, the reactive power is expressed as:

$$\hat{q}_{est} = \sigma L_s \omega_r \left({i_{sd}}^2 + {i_{sq}}^2 \right) + \omega_r \frac{{L_m}^2}{L_r} {i_{sd}}^2 \tag{4.46}$$

The adaptation scheme for reactive power based MRAS is derived as follows:

$$\hat{\omega}_r = \left(K_{p\omega} + \frac{K_{i\omega}}{p}\right)\varepsilon_\omega \tag{4.47}$$

Where

$$\varepsilon_\omega = q_{ref} - \hat{q}_{est} \tag{4.48}$$

Reactive power based MRAS offers robustness against stator resistance variation and also avoids the problems of the integrator. However, this scheme suffers the problem of stability in the regenerative mode. Moreover, reactive power nearly vanishes at speeds close to zero.

4.7 CONCLUSION

In this chapter different types of speed estimation techniques for sensor-less vector control of induction machine are presented. Among different sensorless techniques, open-loop estimators and MRAS based observers are discussed in detail as these offer simple implementation and require less computation effort as compared to other methods. MRAS schemes are classified as rotor flux, back e.m.f and reactive power based MRAS schemes depending upon the error vector of speed tuning signal. Among these rotor-flux based MRAS has high stator resistance parameter sensitivity while the reactive power MRAS is insensitive to stator resistance variations. Back e.m.f MRAS has low noise immunity due to differentiation as compared to others. Back e.m.f and reactive power MRAS have stability problems at low stator frequencies as the back e.m.f and reactive power quantities vanishes at low and zero speed.

CHAPTER 5: SIMULATION OF SPEED ESTIMATORS

5.1 INTRODUCTION

In the previous chapter, different types of speed estimation techniques for sensor-less vector control of induction machine were presented in detail. In this chapter, the rotor flux based MRAS and back e.m.f based MRAS techniques are simulated for sensor-less vector control of 2HP and 30HP motors in Matlab/Simulink environment using SPS toolbox in the discrete time frame. Parameters of the machines are tabulated in the Table I in Appendix I.

The Simulink model of sensor-less vector control is shown in Fig. 5.1 and Fig. 5.2 where the output of the speed estimator is used as speed feedback to the drive system in closed loop sensor-less mode of operation.

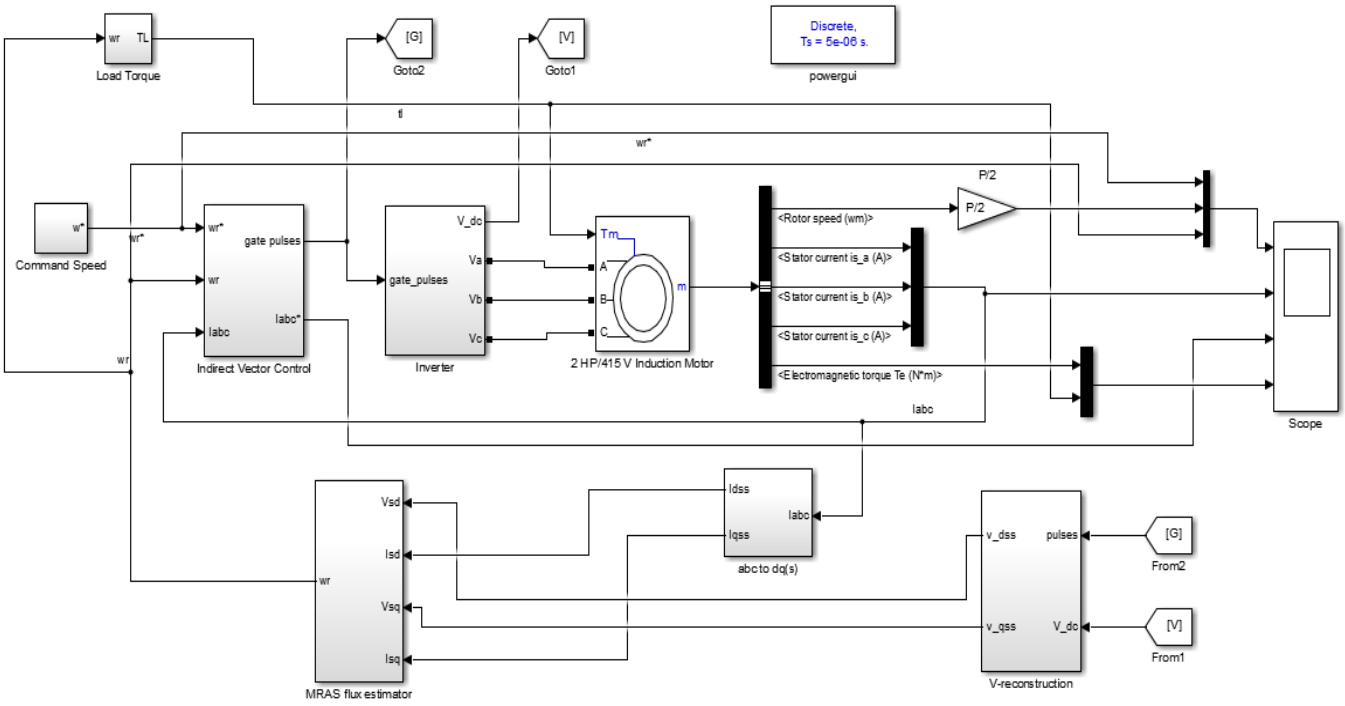

Fig. 5.1 Simulation model of sensor-less vector control of IM drive

Open loop Estimator

In open-loop estimator, the measured stator voltages and currents are used to first estimate the flux linkage components from which the speed is estimated. The Simulink model of open-loop estimator is shown in Fig. 5.2

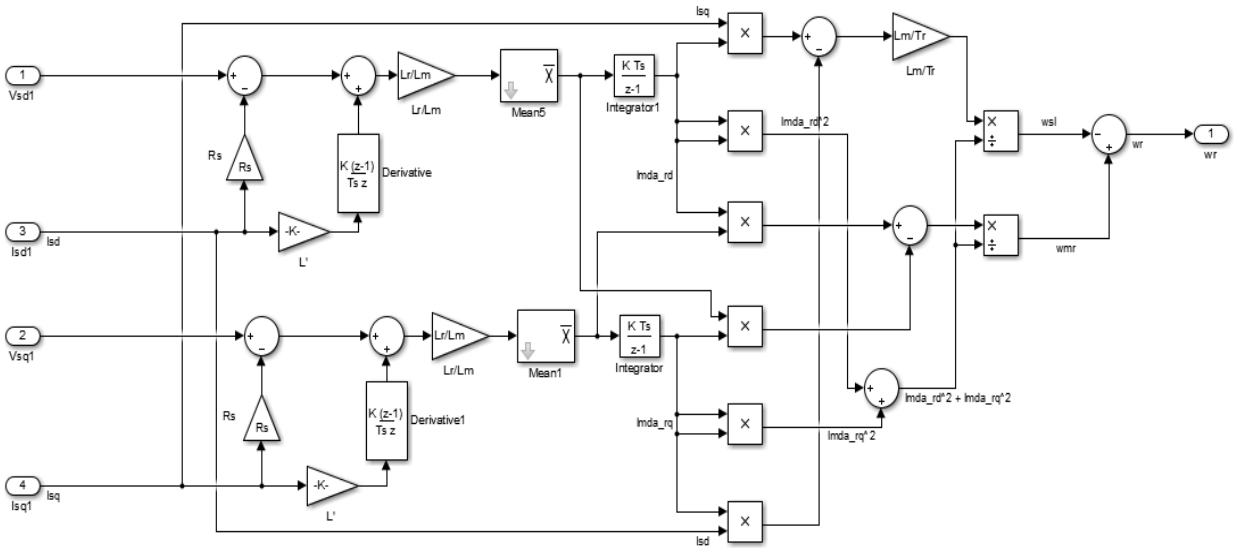

Fig. 5.2 Simulation model of open-loop estimator

Rotor Flux based MRAS

The Simulink model of rotor flux based MRAS is shown in Fig. 5.3 which consists of a reference model, adaptive model and PI controller as an adaptation scheme which generates the estimated speed. In the reference model, the rotor flux ($\overline{\Psi}_r$) is calculated from measured stator voltages and currents and in adaptive model, the rotor flux ($\widehat{\Psi}_r$) is calculated from the measured currents and estimated speed. The error (ε_r) between these rotor flux signals (state variables) is passed to PI controller to estimate the rotor speed.

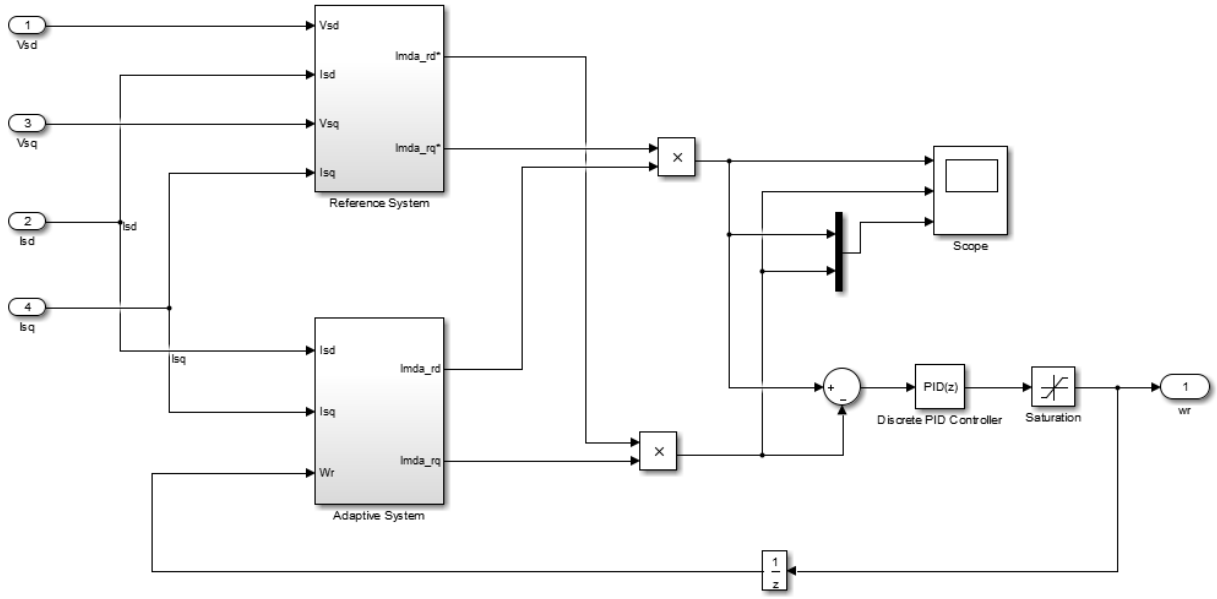

Fig. 5.3 Simulation model of rotor-flux based MRAS

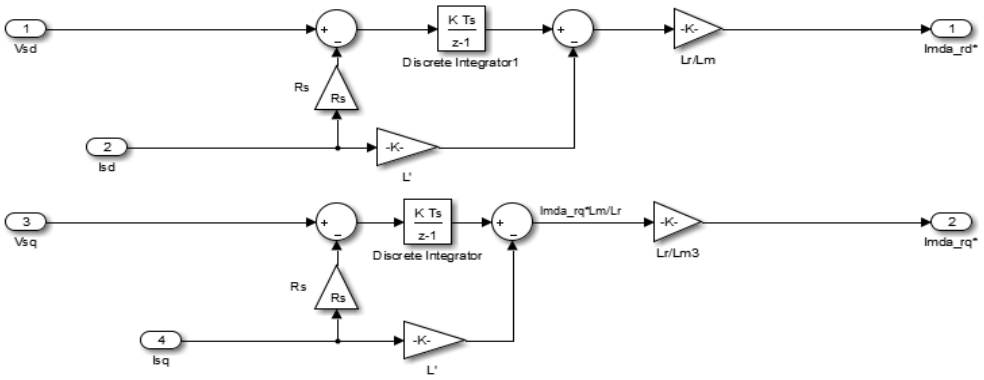

Fig. 5.4 Reference model of rotor-flux based MRAS

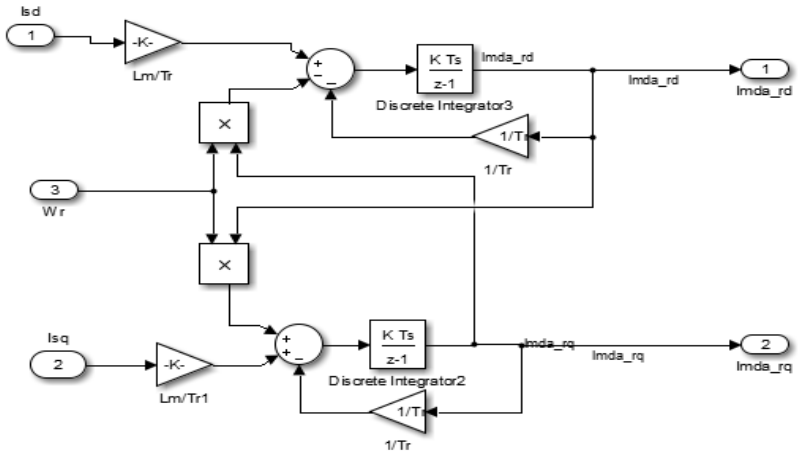

Fig. 5.5 Adaptive model of rotor-flux based MRAS

Back e.m.f based MRAS

Back e.m.f based MRAS speed estimator consists of a reference model, adaptive model and PI controller as an adaptation scheme which generates the estimated speed. In the reference model, the back e.m.f ($\bar{e}_m$) is calculated from measured stator voltages and currents and in adaptive model, the rotor flux ($\hat{e}_m$) is calculated from the measured currents and estimated speed. The error (ε_r) between these rotor flux signals (state variables) is passed to PI controller to estimate the rotor speed. Since voltage-source inverter is used in the simulation system, $i_s = i_s^*$, so the input current i_s to reference model is replaced with i_s^* to avoid noise problem of differentiation. The Simulink models of the reference and the adaptive models are shown in Fig 5.6 and Fig. 5.7.

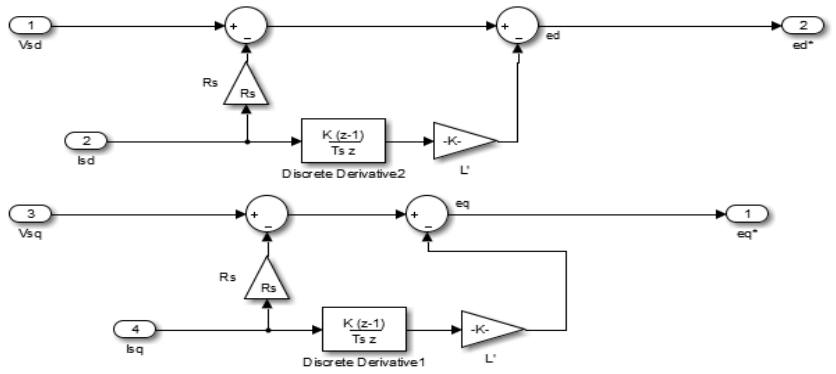

Fig. 5.6 Reference model of back-emf based MRAS

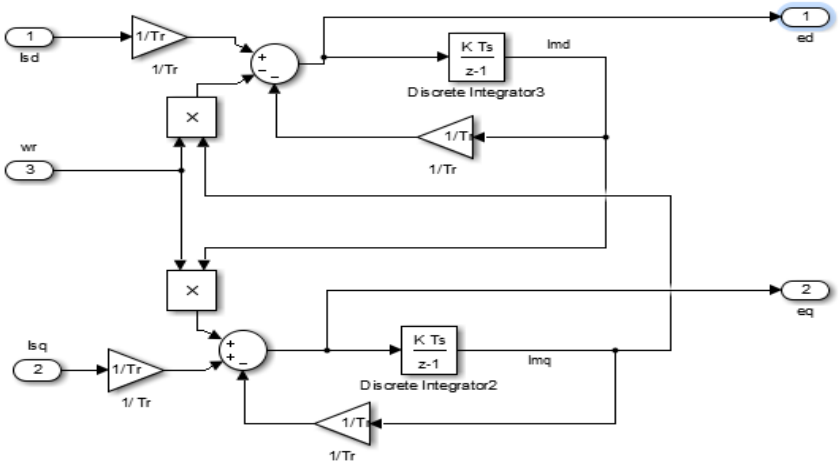

Fig. 5.7 Adaptive model of back-emf based MRAS

5.2 SIMULATION RESULTS

Simulation of Sensorless Vector Controlled IM drive has been discussed in the previous sections. In this section, the simulation results of open-loop, rotor-flux and back e.m.f based MRAS are compared for 2Hp induction motor and the parameters are listed in Appendix I. The dynamic performance of the indirect vector control drive using different speed estimation techniques are plotted at different operating conditions such as starting, speed reversal and load perturbation. Then the two MRAS techniques are compared for their sensitivity towards stator resistance variation. The speed response of the drive system for all the speed observer techniques is shown in Fig 5.8.

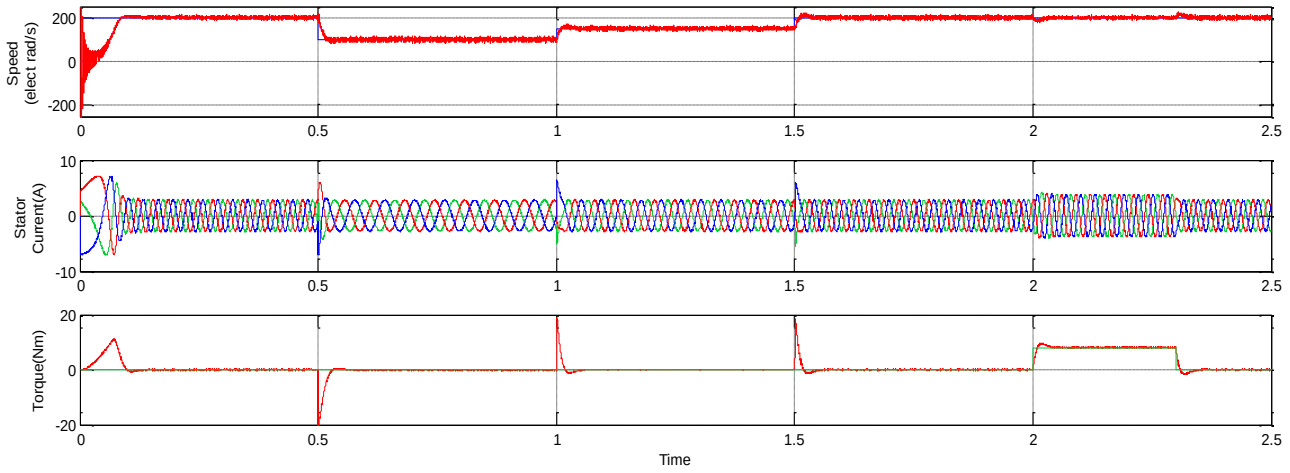

(a)

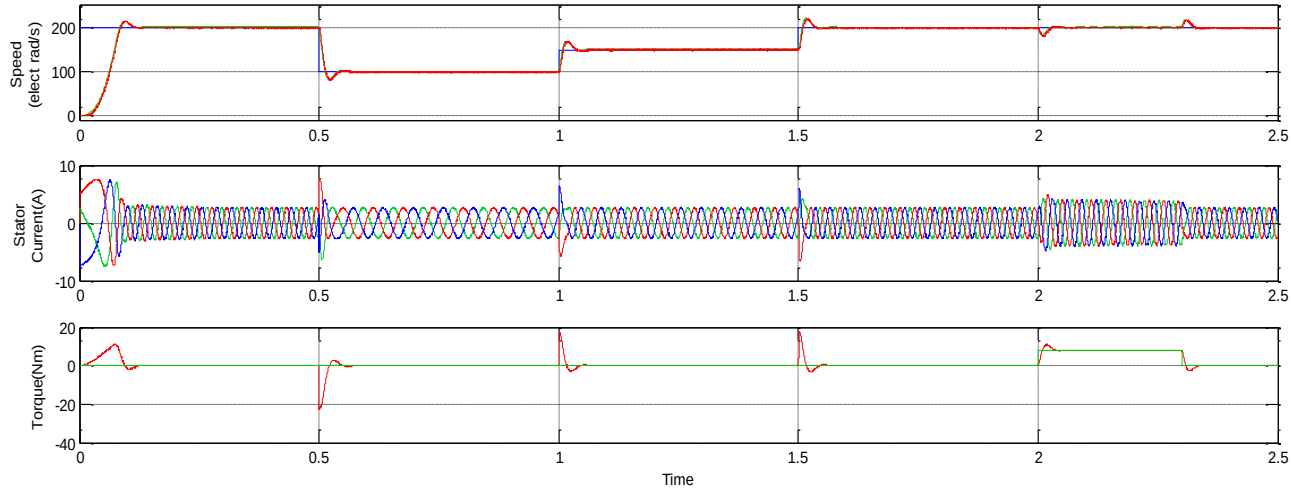

(b)

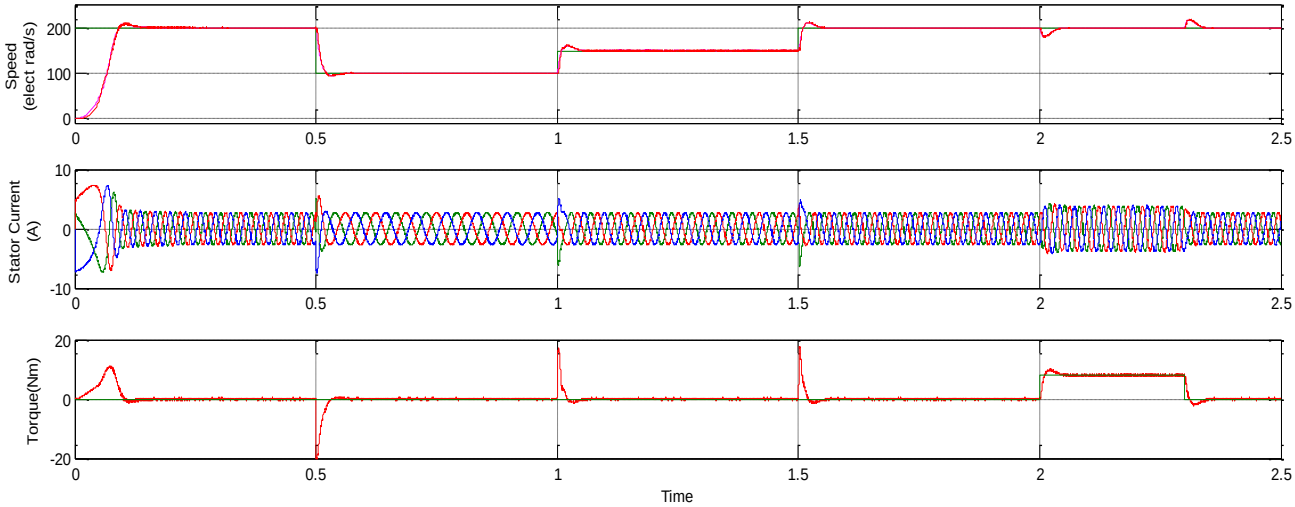

(c)

Fig 5.8. Response of sensor-less induction motor drive using (a) Open-loop estimator (b) Rotor-flux based MRAS (c) Back e.m.f based MRAS

The magnified response of the motor dynamics at different instants is shown in Figure 5.9 to Fig 5.11. The motor is started with a reference speed of 200 electrical rad/s at no-load torque. The speed response of the drive during starting is shown in Fig. 5.9 for all the speed observers and is compared with the performance of the drive when speed is sensed directly. At the motor starting we notice an overshoot in the open-loop estimator while it is absent in MRAS based techniques. The peak overshoot and speed oscillations in the back-emf MRAS are low as compared to other techniques. The back-emf MRAS shows better tracking capability due to the elimination of the pure integration process in the reference model.

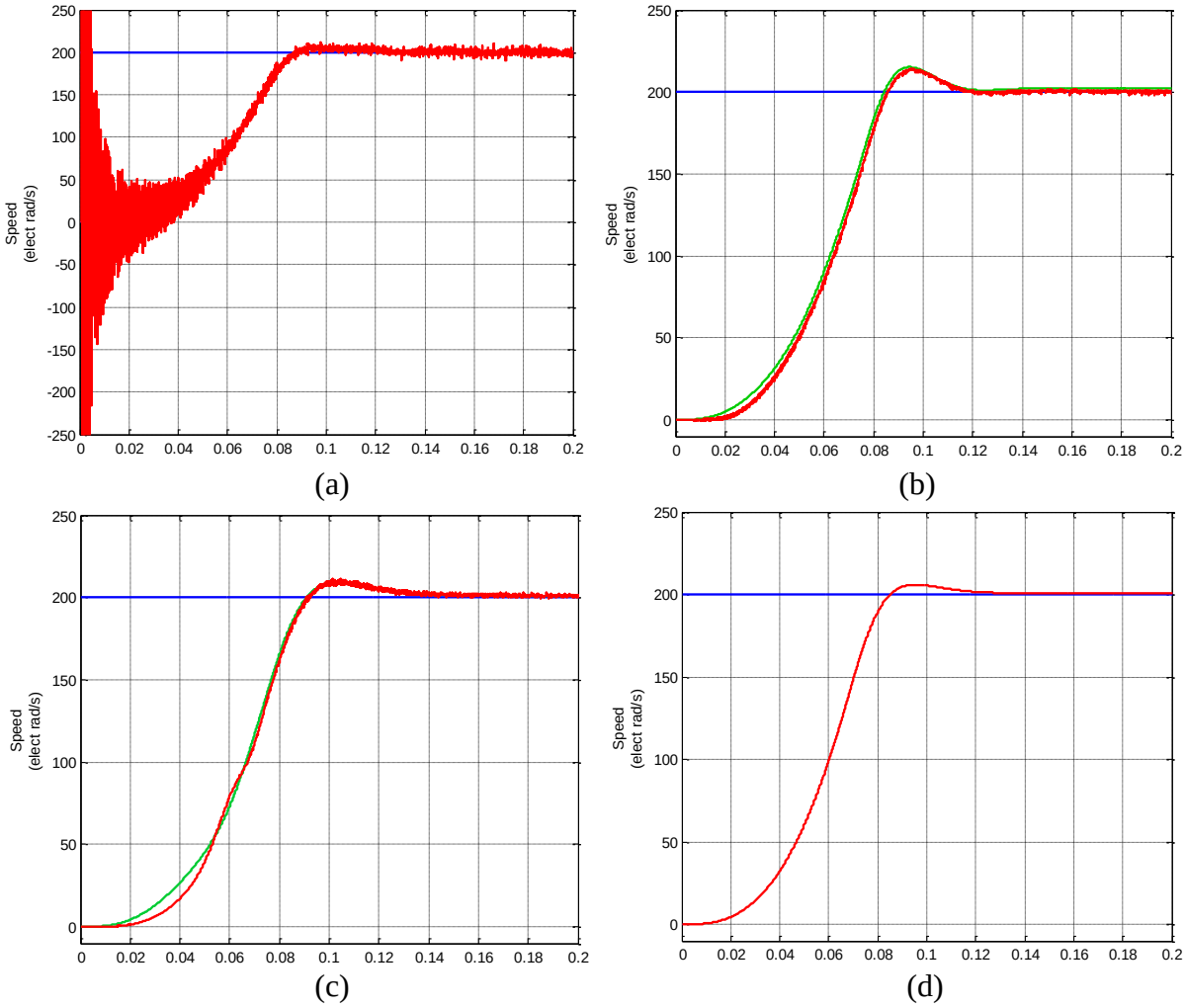

Fig 5.9. Speed Response during starting for (a) Open-loop estimator (b) Rotor-flux based MRAS (c) Back e.m.f based MRAS (d) With speed sensor

(Light green - actual speed, Red-estimated speed)

The reference speed of the drive is changed from 200 electrical rad/s to 100 rad/s; the performance of the drive during speed change is shown in Fig 5.10 for all the speed observers. The back-emf based MRAS shows better speed response as compared to other schemes in terms of peak overshoot, speed oscillations and settling time and its response is comparable to the drive having speed sensor as feedback.

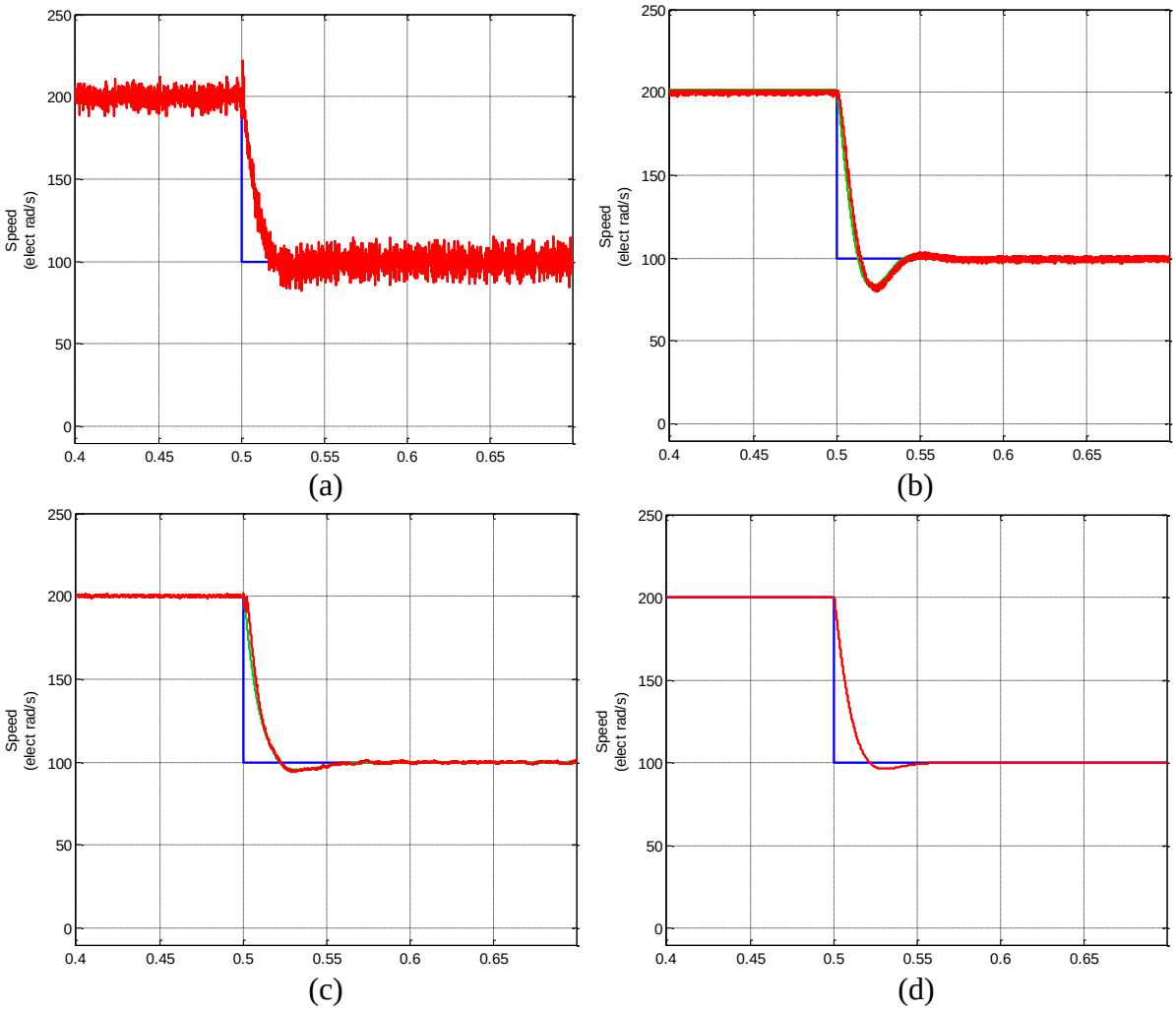

Fig 5.10. Speed Response during speed change from 200 rad/s to 100 rad/s for (a) Open-loop estimator (b) Rotor-flux based MRAS (c) Back e.m.f based MRAS (d) With speed sensor (Light green - actual speed, Red-estimated speed)

The load on the motor is increased from no-load to 80% on the rated value at time t=2s and the decreased from 80% to no-load at t=2.3s to study the load torque rejection capability of the drive. In general, the load disturbance can change the machine parameters and increase the level of nonlinearity. The speed response of the drive during 80% change in load on the motor is shown in Fig 5.11 for all the speed observers. The back-emf based MRAS shows

better dynamic and steady state performance with negligible error between the estimated speed and the actual motor speed as shown in Fig. 5.11 (c).

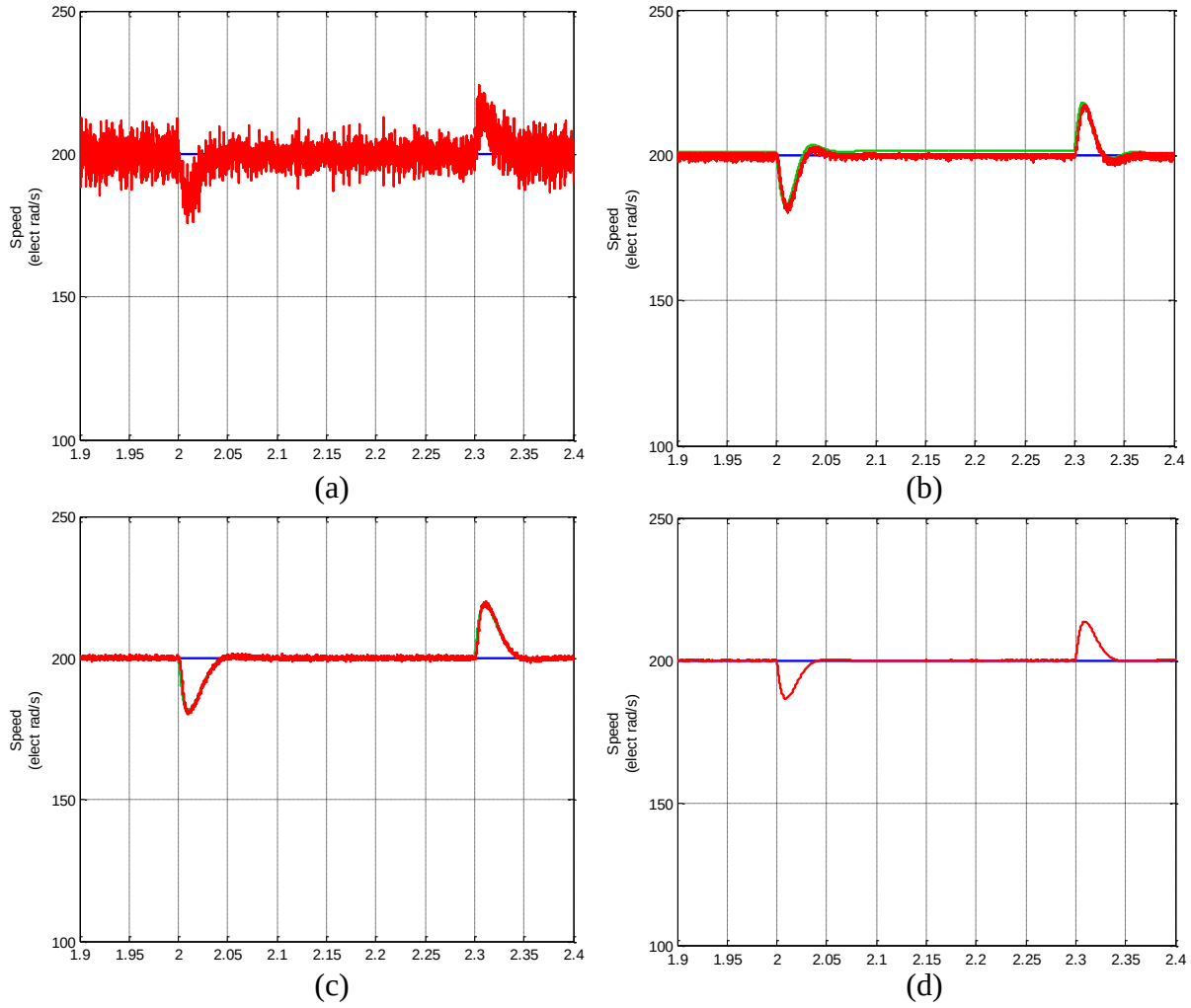

Fig 5.11. Speed Response during load change from no-load to 80% at t=2s and from 80% to no-load at t=2.3s for (a) Open-loop estimator (b) Rotor-flux based MRAS (c) Back e.m.f based MRAS (d) With speed sensor

(Light green - actual speed, Red-estimated speed)

5.3 STATOR RESISTANCE VARIATION

The value of the measured stator resistance which is used in the reference model of the rotor-flux and back e.m.f based MRAS is changed from its actual value to test the sensitivity of both the techniques towards stator resistance variations. Thus, to fit that purpose, the values of parameter in the IM are kept unchanged while the values of the estimators are varied from its rated value. The reference speed is changed from elect 100rad/s to 200rad/s and the speed

response is analyzed at R_s'=1.1 R_s , R_s'=1.2 R_s and R_s'=1.2 R_s. The situation is depicted from Fig. 5.12 to Fig. 5.14.

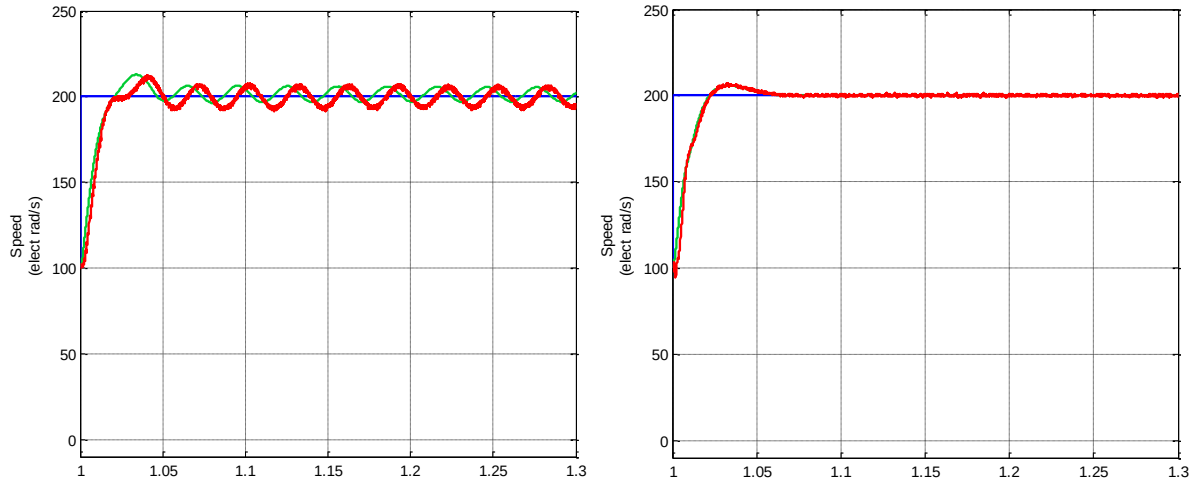

(a) (b)

Fig 5.12: Speed Response at R_s'=1.1R_s for (a) Rotor-flux and (b) Back e.m.f based MRAS

(Light green - actual speed, Red-estimated speed)

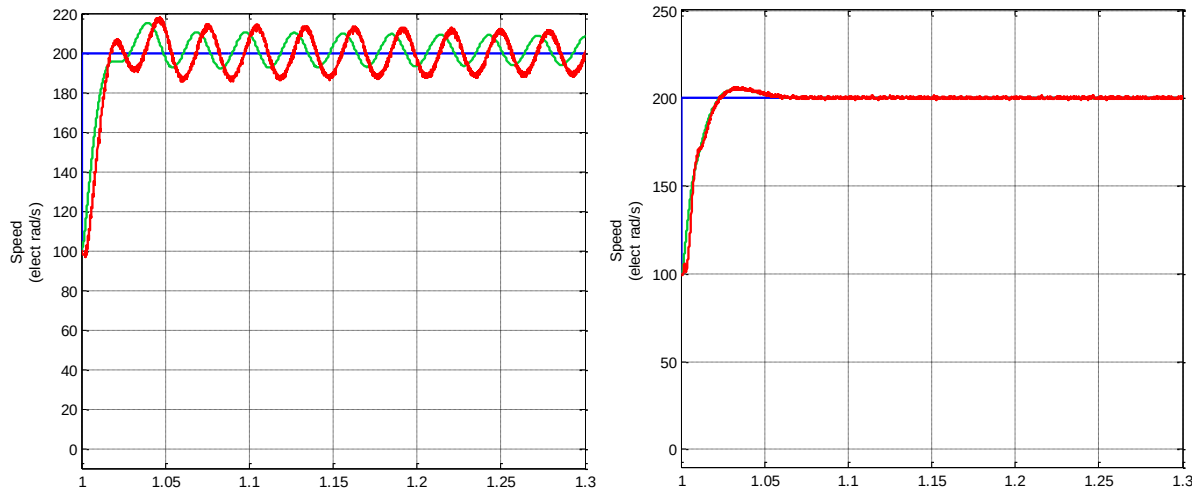

(a) (b)

Fig 5.13: Speed Response at R_s'=1.2R_s for (a) Rotor-flux and (b) Back e.m.f based MRAS

(Light green - actual speed, Red-estimated speed)

As it can be observed from Fig 5.12 to Fig 5.14, the back-e.m.f based MRAS is less parameter dependent as compared to the rotor-flux based MRAS. It shows that back-e.m.f based MRAS scheme is more robust to parameters variations since no significant changes in estimated speed can be noted prior to the variations even at 50% change in stator resistance.

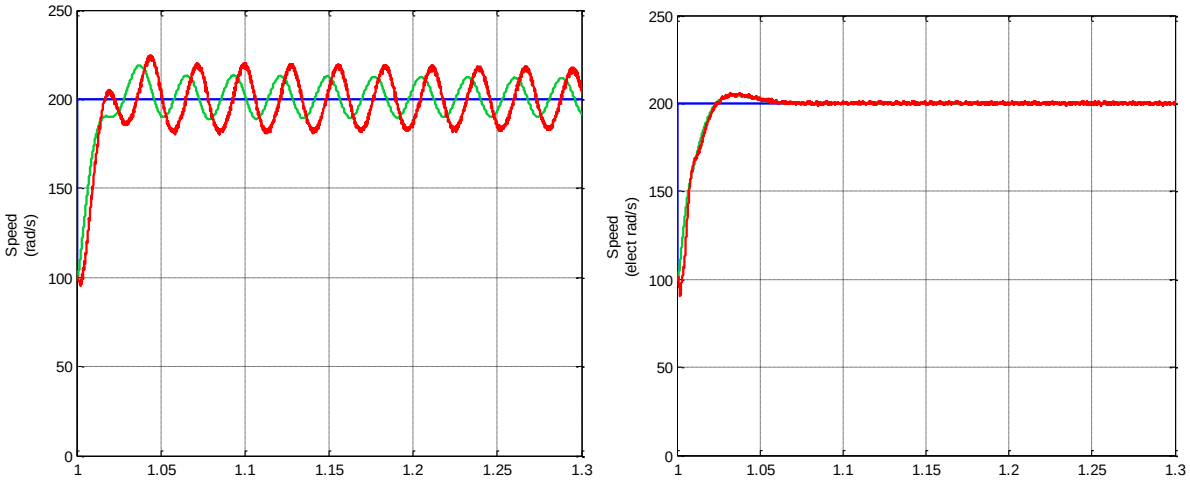

(a) (b)

Fig 5.14: Speed Response at $R_s'=1.5R_s$ for (a) Rotor-flux and (b) Back e.m.f based MRAS (Light green - actual speed, Red-estimated speed)

Table I. Performance comparison of MRAS observers based induction motor drive and the drive having the speed sensor.

Operating Condition	***Parameter***	***Rotor Flux MRAS***	***Back-emf MRAS***	***With Sensor***
During Starting	%Overshoot/ Undershoot	7.5	5	4
	Settling Time(s)	0.17	0.14	0.12
Change in Reference speed	%Overshoot/ Undershoot	15	7	4
	Settling Time(s)	0.06	0.05	0.04
Increase in Load Torque	%Overshoot/ Undershoot	10	8.5	8
	Settling Time(s)	0.05	0.04	0.03

5.3 CONCLUSION

The sensorless speed estimation scheme is implemented on indirect vector control of induction motor drive at various operating conditions such as starting with reference speed of electrical 200 rad/s, speed change from 200 rad/s to 100 rad/s and change in load torque by 80% of rated value. An overshoot in the motor starting is observed in the open-loop estimator while it is absent in MRAS based techniques. The back-emf MRAS shows better tracking capability as compared to rotor-flux based MRAS due to the elimination of the pure integration process in the reference model. The back-emf based MRAS shows better dynamic and steady state performance with negligible error between the estimated speed and the actual motor speed. Also, the back-e.m.f based MRAS scheme is less parameter dependent as compared to other techniques, showing no significant changes in estimated speed when stator resistance value is changed by 50%.

CHAPTER 6: CONCLUSION AND FUTURE SCOPE

A speed sensor is often used in an IM drive for speed measurement in closed loop operation. The speed sensing devices are not reliable, difficult to install in a hostile environment, adds extra cost and complexity to the motor. Speed sensorless vector control offer many advantages. Extensive literature study on vector control of induction machine with and without speed sensor was carried out. Among different speed estimation techniques, MRAS based observers and open-loop estimators were implemented and discussed in detail due to their simple structure and low computational effort. In open loop estimators, the parameter variations have significant influence on the performance of the drive both in transient and steady states. The accuracy is poor at low speeds and the drive may suffer from instability problem. But in comparison the closed loop estimators are more robust to parameter changes and noise.

The closed loop performance of the indirect vector control drive was simulated on 2HP and 30HP motors to validate the indirect vector control model. The detailed results of the simulation were presented in terms of starting performance, speed reversal and load perturbation.

Simulation study using MATLB/Simulink was carried out to test the performance of rotor-flux based MRAS, back-emf based MRAS and open-loop estimator on the indirect vector control IM drive fed by two level voltage source inverter. Simulation results on sensorless control show that the adaptive MRAS based observers have better steady state and transient performance as compared to open loop estimator. The back-emf MRAS shows better tracking capability as compared to rotor-flux based MRAS due to the elimination of the pure integration process in the reference model. The back-emf based MRAS shows better dynamic and steady state performance with negligible error between the estimated speed and the actual motor speed. Also, the back-e.m.f based MRAS scheme is less parameter dependent as compared to other techniques, showing no significant changes in estimated speed when the stator resistance value is changed by 50%.

Future Scope

- At low speeds, due to the continuous variations in machine parameters and non-linearities present in the inverter, fixed gain PI controllers do not provide the required

performance. Replacement of fixed gain PI controller in adaptation scheme with artificial intelligent techniques to improve the performance of speed observers at low speed.

- Further improvement in the sensorless drive can implemented by using emerging topologies of multi-level inverters.
- Use of stator resistance estimation in the rotor-flux based MRAS as the stator resistance variation with machine temperatures is the serious problem at low speed.
- Implementation of new X-MRAS based speed estimator which eliminates the requirement of both flux estimation and derivative operations which mainly affects the performance of the drive.

REFERENCES

[1]. W. Leonard, “Control of Electric Drives”, New Delhi, Narosa Publications, 1985.

[2]. P.C. Krause, Analysis of Electrical Machinery, Prentice Hall, 1985.

[3]. Lipo, Thomas A. "Recent Progress in the Development of Solid State AC Motors Drives." (1987): 125.

[4]. J. Jee-Hoon, J. Gang-Youl and K. Bong-Hwan, “Stability improvement of V/f controlled induction motor drive systems by a dynamic current compensator”, IEEE Transactions on Industrial Electronics, 2004.

[5]. P.Vas, “Vector Control of AC Machines”, Oxford University Press, 1990.

[6]. P.Vas, “Sensorless Vector Control and Direct Torque Control”, Oxford University Press, New York, 1998.

[7]. F. Blaschke, “The Principle Of Field Orientation As Applied To New Transvector Closed-Loop Control System For Rotating-Field Machines*,” Siemens Review*, vol.34, no.3, pp. 217-220, May 1972.

[8]. B.N.Singh, “Investigation of vector control induction motor drive”, Ph.D dissertation, Dept. of Elec. Eng., Indian Institute of Technology, Delhi, India, 1995.

[9]. Gabriel, R., and W. Leonhard. "Microprocessor control of induction motor."*IEEE/IAS Int. Sem. Power Conv. Conf. Rec*. 1982.

[10]. Leonhard, W. "’Control of AC Machines with the help of Microelectronics,’."*Proc. IFAC Symp. on Control In Power Elec. and Elec. Drives*. 1983.

[11]. Sathikumar, S.; Vithayathil, Joseph, "Digital Simulation of Field-Oriented Control of Induction Motor," in *Industrial Electronics, IEEE Transactions on* , vol.IE-31, no.2, pp.141-148, May 1984.

[12]. Matsuo, Takayoshi, and Thomas Lipo. "A rotor parameter identification scheme for vector-controlled induction motor drives." *Industry Applications, IEEE Transactions on* 3 (1985): 624-632.

[13]. Takahashi, I.; Noguchi, T., "A New Quick-Response and High-Efficiency Control Strategy of an Induction Motor," in *Industry Applications, IEEE Transactions on* , vol.IA-22, no.5, pp.820-827, Sept. 1986.

[14]. M. Depenbrock, "Direct self-control (DSC) of inverter-fed induction machine," in *IEEE Transactions on Power Electronics*, vol. 3, no. 4, pp. 420-429, Oct 1988.

[15]. van der Broeck, H.W.; Skudelny, H.-C.; Stanke, G.V., "Analysis and realization of a pulsewidth modulator based on voltage space vectors," in *Industry Applications, IEEE Transactions on* , vol.24, no.1, pp.142-150, Jan/Feb 1988.

[16]. Daboussi, Z.; Mohan, N., "Digital simulation of field-oriented control of induction motor drives using EMTP," in *Energy Conversion, IEEE Transactions on* , vol.3, no.3, pp.667-673, Sep 1988.

[17]. Ho, Edward YY, and Paresh C. Sen. "A microcontroller-based induction motor drive system using variable structure strategy with decoupling." *Industrial Electronics, IEEE Transactions on* 37.3 (1990): 227-235.

[18]. Dakhouche, K., et al. "Modelling of microcomputer-controlled induction machine." *Industrial Electronics Society, 1990. IECON'90., 16th Annual Conference of IEEE*. IEEE, 1990.

[19]. Bose, Bimal K. "Power electronics and motion control-technology status and recent trends." *Industry Applications, IEEE Transactions on* 29.5 (1993): 902-909.

[20]. Fodor, D.; Katona, Z.; Szesztay, E., "Field-oriented control of induction motors using DSP," in *Computing & Control Engineering Journal* , vol.5, no.2, pp.61-65, April 1994.

[21]. Fodor, D., Z. Katona, and E. Szesztay. "Digitized vector control of induction motor with /DSP." *Industrial Electronics, Control and Instrumentation, 1994. IECON'94., 20th International Conference on*. Vol. 3. IEEE, 1994

[22]. Vas, P., A. F. Stronach, and M. Neuroth. "DSP-controlled intelligent high-performance AC drives: present and future." (1995): 7-7.

[23]. Raghavendiran, T. A., and David P. Job. "PC based rotor flux oriented control of induction motors using DSP." *Power Electronics, Drives and Energy Systems for Industrial Growth, 1996., Proceedings of the 1996 International Conference on*. Vol. 1. IEEE, 1996.

[24]. R. Krishnan and F. C. Doran, "Study of Parameter Sensitivity in High-Performance Inverter-Fed Induction Motor Drive Systems", IEEE Transactions on Industry Applications, 1987.

[25]. Holtz, J.: 'Sensorless control of induction machines-with or without signal injection?', IEEE Trans. Ind. Electron., 2006, 53, pp. 7–30

[26]. T.Ohtani, N.Takada, K.Tanaka, "Vector Control of Induction Motor without Shaft Encoder," IEEE Trans. IA, VoI.28, No.l, pp.157-164, 1992.

[27]. C.Schauder, "Adaptive Speed Identification for Vector Control of Induction Motors without Rotational Transducers," IEEE IAS, pp.493-499, 1989.

[28]. K.Rajashekara, A.Kawamura, K.Matsuse, "Speed Sensorless Control of Induction Motors," IEEE Press.

[29]. Cirrincione, M., Pucci, M., Cirrincione, G., Capolino, G.A.: 'A new adaptive neural integrator for improving open-loop speed estimators in induction machine drives'. 35th Annual Power Electronics Specialists Conf. IEEE, June 2004, vol. 5, pp. 3342–3346

[30]. Shoudao, H., Yaonan, W., Jian, G., Jiantao, L., Sihai, Q.: 'The vector control based on MRAS speed sensorless induction motor drive'. Fifth World Congress Intelligent Control and Automation, June 2005, vol. 5, pp. 4550–4553

[31]. Vas, P.: 'Sensorless vector and direct torque control' (Oxford University Press, New York, 1998)

[32]. Rehman, H.U., Derdiyok, A., Guven, M.K., Longya, X.: 'An MRAS scheme for on-line rotor resistance adaptation of an induction machine'. Proc. Power Electronics Specialist Conf., Vancouver, 2001, vol. 2, pp. 817–822

[33]. Schauder, C.: 'Adaptive speed identification for vector control of induction motors without rotational transducers'. IAS Annual Meeting, USA, (IEEE Transactions on Industry Applications), October (September/October)1989 (1992), vol. 28, no. 5, pp. 493–499(1054–1061)

[34]. Kim, Y.R., Sul, S.K., Park, M.H.: 'Speed sensorless vector control of induction motor using extended Kalman filter', IEEE Trans. Ind. Appl., 1994, 30, (5), pp. 1225–1233
[35]. Pongam, S., Sangwongwanich, S.: 'Stability and dynamic performance improvement of adaptive full-order observers for sensorless PMSM drive', IEEE Trans. Power Electron., 2012, 27, pp. 588–600
[36]. Vas, P., Stronach, A.F., Rashed, M., Neuroth, M.: 'Implementation of ANN-based sensorless induction motor drives'. Ninth Int. Conf. Electrical Machines and Drives, 1999, pp. 329–333
[37]. Khan, M.R., Iqbal, I., Mukhtar, A.: 'MRAS-based sensorless control of a vector controlled five-phase induction motor drive', Electr. Power Syst. Res., 2008, 78, (8), pp. 1311–1321
[38]. Peng, F.Z., Fukao, T.: 'Robust speed identification for speed sensorless vector control of induction motors', IEEE Trans. Ind. Appl., 1994, 30, (5), pp. 1234–1240
[39]. Rashed, M., Stronach, A.F.: 'A stable back-EMF MRAS-based sensorless low-speed induction motor drive insensitive to stator resistance variation', IEEE lectr. Power Appl. Proc., 2004, 151, (6), pp. 685–693
[40]. Maiti, S., Chakraborty, C., Hori, Y., Ta, C.M.: 'Model reference adaptive controller-based rotor resistance and speed estimation techniques for vector controlled induction motor drive utilizing reactive power', IEEE Trans. Ind. Electron., 2008, 55, (2), pp. 594–601
[41]. Ta, C.M., Uchida, T., Hori, Y.: 'MRAS-based speed sensorless control for induction motor drives using instantaneous reactive power'. 27th Annual Conf. IEEE Industrial Electronics Society, 2001, vol. 2, pp. 1417–1422
[42]. Ahmad Razani Haron, Nik Rumzi Nik Idris,"Simulation of MRAS-based Speed Sensorless Estimation of Induction Motor Drives using MATLAB/SIMULINK", First International Power and Energy Coference PECon 2006
[43]. Tamai, S., Sugimoto, H., Yano, M.: 'Speed sensorless vector control of induction motor applied model reference adaptive system'. Conf. Record IEEE/MS Annual Meeting, 1985, pp. 613–620
[44]. Armstrong, G.J., Atkinson, D.J., Acarnley, P.P.: 'A comparison of estimation techniques for sensorless vector controlled induction motor drives'. Int. Conf. Power Electronics Drive Systems, May 1997, vol. 1, pp. 110–116

Appendix-A

Table II. Parameters of 30hp and 2hp induction motors used in the simulation

Parameter	***30HP***	***2HP***
$V_{rms}(L-L)$	415V	415V
N_{rated} ***(rpm)***	1440	1440
Rs (Ω)	0.251	5.4
Rr (Ω)	0.249	3.1093
Lls (H)	0.001397	0.02840
Llr (H)	0.001397	0.02840
Ls (H)	0.042997	0.41755
Lr (H)	0.042997	0.41755
Lm (H)	0.0416	0.38915
J (kg m^2)	0.305	0.004363641
P	4	4
Base flux (stator)	1.073Wb	1.078Wb

Appendix-B

The values of parameter of speed controllers considered in the investigation Simulation analysis are as follows:

Speed Controller Parameters (For 30HP VCIMD):

KP = 20 KI = 0.5

Speed Controller Parameters (For 2HP VCIMD):

KP = 0.3 KI = 0.002

PI Controller parameters in Rotor-flux based MRAS estimator

KP = 600 KI = 300

PI Controller parameters in Back-emf based MRAS estimator

KP = 0.01 KI = 5